

NASA TM-83126



3 1176 00168 7145

NASA Technical Memorandum 83126

NASA-TM-83126 19810016896

PREDICTION OF TRANSONIC FLUTTER FOR A
SUPERCritical WING BY MODIFIED STRIP
ANALYSIS AND COMPARISON WITH EXPERIMENT

E. CARSON YATES, JR., ELEANOR C. WYNNE,
MOSES G. FARMER, AND ROBERT N. DESMARAIS

MAY 1981

MAY 1981

National Aeronautics and
Space Administration

Langley Research Center
Hampton, Virginia 23665



NF00388

PREDICTION OF TRANSONIC FLUTTER FOR A SUPERCRITICAL WING
BY MODIFIED STRIP ANALYSIS AND COMPARISON WITH EXPERIMENT

E. Carson Yates, Jr.,* Eleanor C. Wynne,**
Moses G. Farmer,† and Robert N. Desmarais‡
NASA Langley Research Center
Hampton, Virginia

Abstract

The experiments of Farmer, Hanson, and Wynne¹ showed that use of a supercritical airfoil can adversely affect wing flutter speeds in the transonic range. Inasmuch as adequate theories for three-dimensional unsteady transonic flow are not yet available, the modified strip analysis published by Yates in 1958³ has been used to predict the transonic flutter boundary for the supercritical wing tested by Farmer, Hanson, and Wynne. The steady-state spanwise distributions of section lift-curve slope and aerodynamic center, required as input for the flutter calculations, were obtained from pressure distributions measured by Harris.² The calculated flutter boundary is in excellent agreement with experiment in the subsonic range. In the transonic range, a "transonic bucket" is calculated which closely resembles the experimental one with regard to both shape and depth, but it occurs at about 0.04 Mach number lower than the experimental one.

Nomenclature

$a_{c,n}$	nondimensional distance from midchord to section aerodynamic center measured perpendicular to elastic axis, positive rearward, fraction of semichord b
b_r	semichord of wing measured perpendicular to elastic axis at spanwise reference station $\eta = 0.75$ ($b_r = 0.14948$ m)
$C_{L_{\alpha,n}}$	section lift-curve slope for a section perpendicular to elastic axis
C_p	pressure coefficient
H	translational displacement of wing at elastic axis, positive downward, fraction of reference semichord b_r
k_{nr}	reduced frequency based on spanwise reference station ($\eta = 0.75$) and on velocity component normal to elastic axis, $b_r \omega / V \cos \Lambda_{ea}$
M	freestream Mach number
m_r	mass of wing per unit span at spanwise reference station ($\eta = 0.75$) ($m_r = 2.57$ kg/m)
q	freestream dynamic pressure
V	freestream speed
X	streamwise distance from local leading edge, fraction of local chord
Y	spanwise station, fraction of semispan

*Aerospace Engineer, Unsteady Aerodynamics Branch, Loads and Aeroelasticity Division

**Mathematician, Unsteady Aerodynamics Branch, Loads and Aeroelasticity Division

†Aerospace Engineer, Configuration Aeroelasticity Branch, Loads and Aeroelasticity Division

‡Aerospace Engineer, Unsteady Aerodynamics Branch, Loads and Aeroelasticity Division

α	angle of attack
η	nondimensional coordinate measured from wing root along elastic axis, fraction of elastic axis length
θ	torsional displacement of wing about elastic axis, positive leading edge up
Λ_{ea}	sweep angle of elastic axis ($\Lambda_{ea} = 40.03^\circ$)
μ_r	mass ratio based on spanwise reference station ($\eta = 0.75$), $m_r / \pi \rho b_r^2$
ρ	freestream density
ω	circular frequency of vibration
ω_r	reference frequency, frequency of first uncoupled torsional mode of wing ($\omega_r = 227.23$ rad/sec)

Introduction

The experiments of Farmer, Hanson, and Wynne,¹ which determined the flutter characteristics of a supercritical wing and a dynamically similar conventional wing having the same planform, showed that use of a supercritical airfoil can adversely affect wing flutter speeds in the transonic range. Although it was evident from aerodynamic data available more than ten years ago² that this adverse effect should occur, the results of Ref. 1 aroused considerable concern, which in turn led to renewed interest in predicting the flutter characteristics of supercritical wings. Inasmuch as conventional lifting-surface theories do not lead to accurately predicted transonic flutter characteristics, and because adequate theories for three-dimensional unsteady transonic flow have not yet been developed, the modified strip analysis, first published by Yates³ in 1958, has been used here to predict the transonic flutter boundary for the supercritical wing (Fig. 1) which was investigated in Ref. 1. McGrew et al⁴ have also calculated flutter characteristics for this wing but by use of subsonic doublet-lattice aerodynamic in combination with an extensive set of "weighting factors."

The modified strip analysis used here has given good flutter results for a broad range of swept and unswept wings at speeds up to hypersonic,⁵ including effects of wing thickness^{6,7} and angle of attack.⁸ In particular, it was used successfully to calculate transonic flutter characteristics for some swept wings with conventional airfoils.⁹

In addition to results calculated for comparison with the experimental data of Ref. 1, results are also shown herein which more broadly define the flutter characteristics of this wing in terms of the variations of flutter parameters with mass ratio at constant Mach number and with Mach number at constant mass ratio.

Flutter Model Parameters

The geometric, elastic, and inertial properties used in the present calculations are measured values for the supercritical-wing flutter model of Ref. 1. The model geometry is shown in Fig. 1a. The frequencies and mode lines of the first six measured natural vibration modes are presented in Fig. 1b, and the modal deflections are given in Fig. 2. The corresponding generalized masses were determined by the method of displaced frequencies.¹⁰

These six measured modes were used in all of the flutter calculations shown herein. Some colateral flutter calculations, made with up to twelve vibration modes calculated with the NASTRAN* finite-element structural analysis, indicated that six modes were sufficient to converge flutter speeds and frequencies within 2 percent. Flutter calculations with the measured modes, however, appeared to converge more rapidly than those with NASTRAN modes. Consequently, the six-measured-mode results presented here are considered to be converged within about 1 percent.

Flutter Analysis

Method

The modified strip analysis³ used here is formulated for wing strips oriented normal to the elastic axis and is based on stripwise application of Theodorsen-type aerodynamics¹¹ in which the lift-curve slope of 2π and aerodynamic center at quarter chord are replaced, respectively, by the lift-curve slope and aerodynamic center for the same strip of the three-dimensional wing at the appropriate Mach number. The downwash collation point, where the downwash induced by the aerodynamic load is set equal to the kinematic downwash, is modified accordingly. The circulation function is modified for compressibility by use of two-dimensional unsteady compressible-flow theory.¹² Further description and discussion of this method are contained in Refs. 3, 5, 9, and 13.

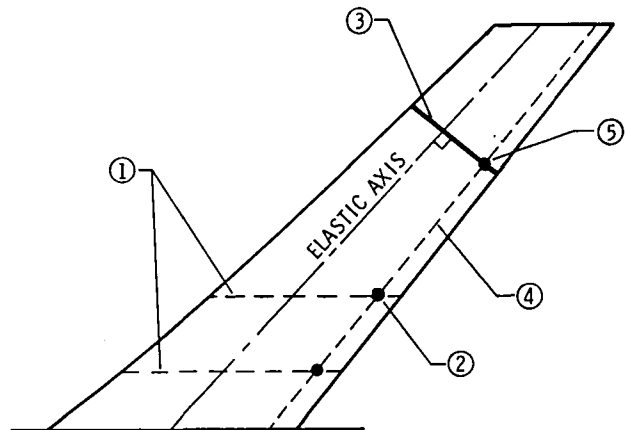
Aerodynamic Parameters

The required spanwise distributions of section lift-curve slope and aerodynamic center were obtained from steady-state surface pressure measurements made by Harris² in the Langley 8-Foot Transonic Pressure Tunnel and in the Langley 16-Foot Transonic Tunnel. Upper- and lower-surface pressures were measured along streamwise wing sections at six stations along the semispan (Figs. 3 and 4). Since the flutter tests were conducted at angles of attack near zero, the pressure data for the two angles of attack nearest zero were selected for use in the flutter calculations. The boundary-layer transition strips on the pressure model were represented also on the flutter model.

Values of section lift-curve slope and section aerodynamic center for 40 wing sections equispaced along the elastic axis and oriented perpendicular to the elastic axis were required as input for the flutter calculations. These values were obtained

by differencing the corresponding values of section lift coefficient and pitching-moment coefficient for the two angles of attack shown on each part of Figs. 3 and 4. The section lift and moment coefficients were calculated by 8-point Gaussian integration of the lifting pressure along each of the 40 wing sections

The procedure for obtaining values of lifting pressure at the eight quadrature abscissas on each of the 40 wing sections from the measured pressures is described in the following discussion and sketch.



SKETCH NOT TO SCALE

- ① Two of six streamwise lines along which pressures were measured
- ② One of eight points on each streamwise line at which pressures were interpolated
- ③ One of 40 wing sections on which lift and moment coefficients were required
- ④ One of eight lines of constant quadrature abscissa
- ⑤ One of eight quadrature points on each of 40 wing sections

Since measured pressures were available only along six streamwise lines (see sketch), it was necessary to interpolate the upper- and lower-surface pressures streamwise (Figs. 3 and 4) for the eight Gaussian-quadrature abscissas using the spline curves shown in these figures. For each of the quadrature abscissas, the resulting six values of lifting pressure (lower-surface pressure minus upper-surface pressure) were spline-interpolated from root to tip, and values were thus obtained at the required 40 wing sections.

The distributions of section lift-curve slope and section aerodynamic center thus obtained are shown in Figs. 5 and 6. The change in the slopes of the curves inboard is caused by use of the dashed planform in Fig. 1 as reference while preserving the section lift and moment values for the wing with glove. The spline-curve extrapolations beyond the aft-most experimental points in Figs. 3 and 4 generally indicate nonvanishing lifting pressures at the wing trailing edge. To examine

*NASTRAN: Registered trademark of the National Aeronautics and Space Administration

the extent to which the calculated flutter characteristics were affected by the pressure-data fairing near the trailing edge, some collateral calculations were made with a Kutta condition imposed to force the lifting pressure to zero at the trailing edge. The resulting changes in calculated flutter characteristics were negligible.

Pressure data² from the tests in the 8-Foot Transonic Pressure Tunnel for Mach numbers up to 1.0 are available for two levels of dynamic pressure at each Mach number. Consequently, it is possible to assess the effect on aerodynamic parameters (and hence on flutter) of static aeroelastic deformation of the pressure model, together with an accompanying change in Reynolds number.* The comparison in Fig. 5f is typical. Increasing the dynamic pressure reduces the lift-curve slope and moves the aerodynamic center forward, especially over the outboard portions of the wing. These changes have opposing effects on flutter speed, and the resulting changes in calculated flutter characteristics are quite minor. Nevertheless, the lower value of dynamic pressure was selected for all of the flutter calculations presented herein because those pressure data should be less affected by deformation than those obtained at the higher dynamic pressure. The effect of the associated change in Reynolds number is considered to be quite small since the previously indicated changes in aerodynamic parameters caused by changing dynamic pressure are in a direction opposite to that anticipated from Reynolds-number change alone.

Mass Ratio

The mass ratios used in flutter calculations made for direct comparison with the experimental flutter data of Ref. 1 were taken from a curve faired through the experimental mass ratios (Fig. 7). Inasmuch as no flutter data were obtained at Mach numbers higher than 1.055, the mass ratio for that Mach number was used for all higher Mach numbers. In addition, mass ratio was varied parametrically up to a value of 98 for each Mach number in order to trace out "slices" of a flutter surface (flutter-speed index as a function of Mach number and mass ratio) such as that discussed in Appendix C of Ref. 6.

Results and Discussion

Values of flutter-speed index and flutter-frequency ratio calculated with mass ratios taken from the curve in Fig. 7 are compared with the experimental data¹ in Figs. 8 and 9, respectively. Agreement between calculated and measured flutter boundaries (Fig. 8) is excellent in the subsonic range. In the transonic range, a "transonic bucket" is calculated which closely resembles the experimental one with regard to both shape and depth. However, the calculated bucket occurs at about

0.04 Mach number lower than the experimental one. The reason for this difference is not known with certainty. There is some indication, however, that the difference may be associated with flutter-model scale effect in the wind tunnel. A limited number of flutter points were measured with a second model of the wing with conventional airfoil¹ but 0.4 as large as that reported in Ref. 1 (and 0.4 as large as the supercritical-wing model). The data for the smaller model showed the bottom of the transonic bucket to be shifted down about 0.04 in Mach number relative to that for the larger model. It is not likely that this difference was caused by the difference in blockage because blockage would be expected to cause the larger model to encounter transonic effects at lower Mach numbers than the smaller model. It is noted that, relative to tunnel dimensions, the pressure model is intermediate in size between the two conventional-airfoil flutter models and smaller than the supercritical wing model.

The calculated flutter frequencies (Fig. 9) are slightly higher than experimental values up to Mach number 0.95, as was the case in Ref. 4. The reason for the somewhat erratic variation between Mach numbers 0.95 and 1.00 (square symbols in Fig. 9) is not clear. In that Mach number range, however, aerodynamic data are available from both the 8-foot tunnel and the 16-foot tunnel. Although the calculated flutter speeds are in good agreement with each other at the two duplicated Mach numbers (M = 0.95 and M = 0.99) (Fig. 8), the flutter frequencies obtained from the 16-foot tunnel data (diamond symbols) are higher and farther from flutter experiment than those calculated with 8-foot tunnel data (square symbols). The cause of this difference is entirely aerodynamic, and this may indicate that there is also a model scale effect on flutter frequency. Relative to tunnel size, the pressure model in the 16-foot tunnel was smallest; the same pressure model in the 8-foot tunnel was intermediate; and the flutter model in the Transonic Dynamics Tunnel was largest. Thus, if extrapolation of flutter frequency with respect to model size is valid, lower calculated flutter frequencies would be expected if the pressure model were the same size as the flutter model relative to tunnel dimensions. This is, of course, speculative and empirical since no physical mechanism to produce this effect is postulated.

The variations of flutter-speed index, flutter-frequency-ratio, and reduced frequency with mass ratio (Fig. 10) are quite conventional and confirm that the upturn in the flutter speed and flutter frequency (Figs. 8 and 9) as Mach number decreases to 0.25 is caused by the accompanying decrease in mass ratio. This effect is illustrated more clearly in Fig. 11 where the calculated flutter characteristics from Figs. 8 and 9 are compared with corresponding values calculated for a constant mass ratio of 27.41 which is the value for Mach number 0.80 from Fig. 7.

Concluding Remarks

Flutter calculations have been made by modified strip analysis for a supercritical wing model for which experimental flutter data and steady-state pressure distributions were previously available. Use of these pressure data to generate aerodynamic

*Reynolds numbers of 2.2×10^6 and 3.3×10^6 at M = 0.90 (based on mean geometric chord) are representative for the 8-foot tunnel tests. The corresponding Reynolds number for the flutter test was near the higher value.

input for the flutter calculations produced a flutter boundary that is in excellent agreement with experiment in the subsonic range. In the transonic range, a "transonic bucket" was calculated which closely resembles the experimental one with regard to both shape and depth, but it occurs at about 0.04 Mach number lower than the experimental one. Some evidence indicates that this shift may be related to differences in model size relative to tunnel size for the pressure model and the flutter model, but this is not conclusive.

Nevertheless, the good results herein for the supercritical wing and good results obtained previously for swept wings with conventional airfoils at subsonic, transonic, and supersonic speeds indicate that the modified strip analysis in conjunction with aerodynamic parameters from steady-state experiments, is still useful for transonic speeds in the absence of validated nonlinear, three-dimensional, unsteady aerodynamic analysis methods.

References

- ¹Farmer, Moses G.; Hanson, Perry W.; and Wynne, Eleanor C.: Comparison of Supercritical and Conventional Wing Flutter Characteristics. NASA TM-72837, 1976.
- ²Harris, Charles D.: Wind-Tunnel Investigation of the Aerodynamic Load Distribution of a Supercritical Wing Research Airplane Configuration. NASA TM X-2469, February 1972.
- ³Yates, E. C., Jr.: Calculation of Flutter Characteristics for Finite-Span Swept or Unswept Wings at Subsonic and Supersonic Speeds by a Modified Strip Analysis. NACA RM L57L10, 1958.
- ⁴McGrew, J. A.; Giesing, J. P.; Pearson, R. M.; Zuhuruddin, K.; Schmidt, M. E.; and Kalman, T. P.: Supercritical Wing Flutter. AFFDL-TR-78-37, March 1978.
- ⁵Yates, E. Carson, Jr.: Modified-Strip-Analysis Method for Predicting Wing Flutter at Subsonic to Hypersonic Speeds. J. Aircraft, Vol. 3, No. 1, February 1966.
- ⁶Yates, E. Carson, Jr.; and Bennett, Robert M.: Use of Aerodynamic Parameters from Nonlinear Theory in Modified-Strip-Analysis Flutter Calculations for Finite-Span Wings at Supersonic Speeds. NASA TN D-1824, July 1963.
- ⁷Yates, E. Carson, Jr.: Subsonic and Supersonic Flutter Analysis of a Highly Tapered Swept-Wing Planform, Including Effects of Density Variation and Finite Wing Thickness, and Comparison with Experiments. NASA TN D-4230, November 1967.
- ⁸Yates, E. Carson, Jr.; and Bennett, Robert M.: Analysis of Supersonic-Hypersonic Flutter of Lifting Surfaces at Angle of Attack. J. Aircraft, Vol. 9, No. 7, July 1972, pp. 481-489.

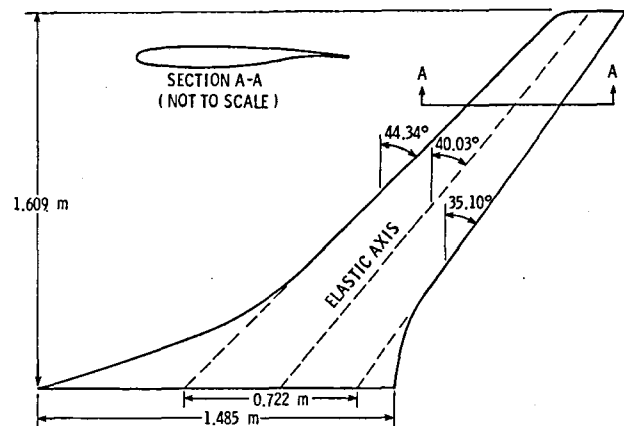
- ⁹Yates, E. Carson, Jr.: Use of Experimental Steady-Flur Aerodynamic Parameters in the Calculation of Flutter Characteristics for Finite-Span Swept or Unswept Wings at Subsonic, Transonic, and Supersonic Speeds. NASA TM X-183, 1959.

- ¹⁰De Vries, G.: Sondage des Systèmes Vibrants par Masses Additionnelles. Rech. Aéronaut., No. 30, Nov.-Dec. 1952, pp. 47-49.

- ¹¹Theodorsen, Theodore: General Theory of Aerodynamic Instability and the Mechanism of Flutter. NACA Rep. 496, 1935.

- ¹²Jordan, P. F.: Aerodynamic Flutter Coefficients for Subsonic, Sonic and Supersonic Flow (Linear Two-Dimensional Theory). R. & M. No. 2932, British A. R. C., 1957.

- ¹³Yates, E. Carson, Jr.: Flutter and Unsteady-Lift Theory. In "Performance and Dynamics of Aerospace Vehicles." NASA SP-258, 1971.

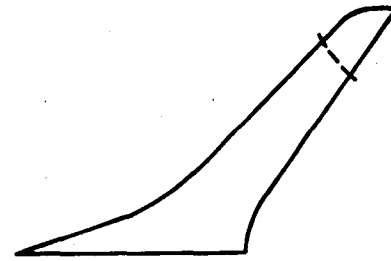


(a) Wing planform.

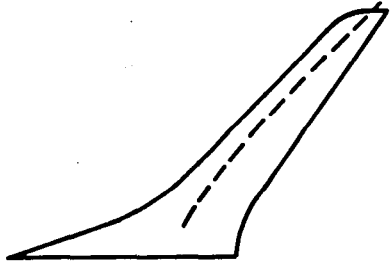
Fig. 1 Supercritical wing flutter model.



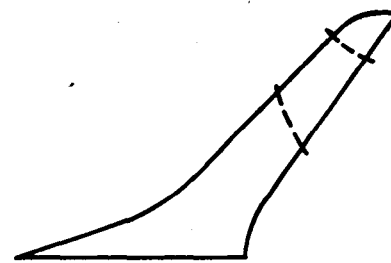
MODE 1, 33.24 rad/sec



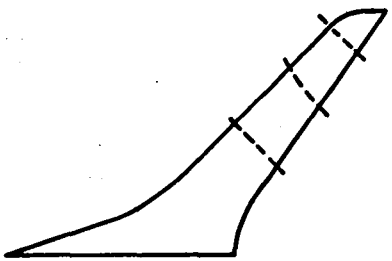
MODE 2, 113.6 rad/sec



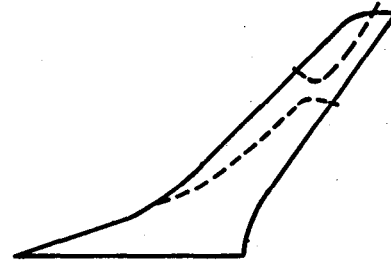
MODE 3, 233.1 rad/sec



MODE 4, 268.9 rad/sec



MODE 5, 461.2 rad/sec



MODE 6, 466.8 rad/sec

(b) Node lines of measured vibration modes.

Fig. 1 Concluded.

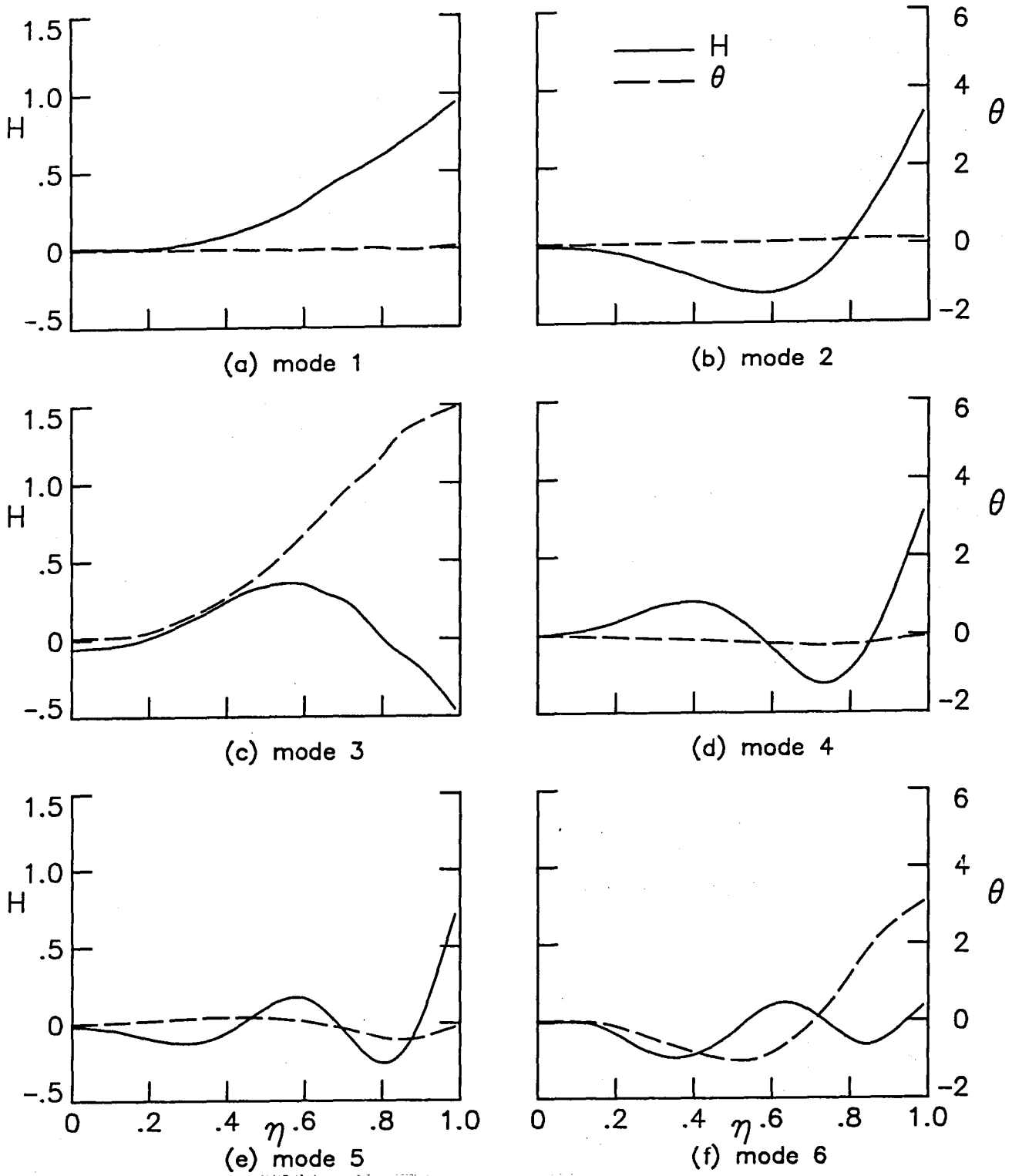
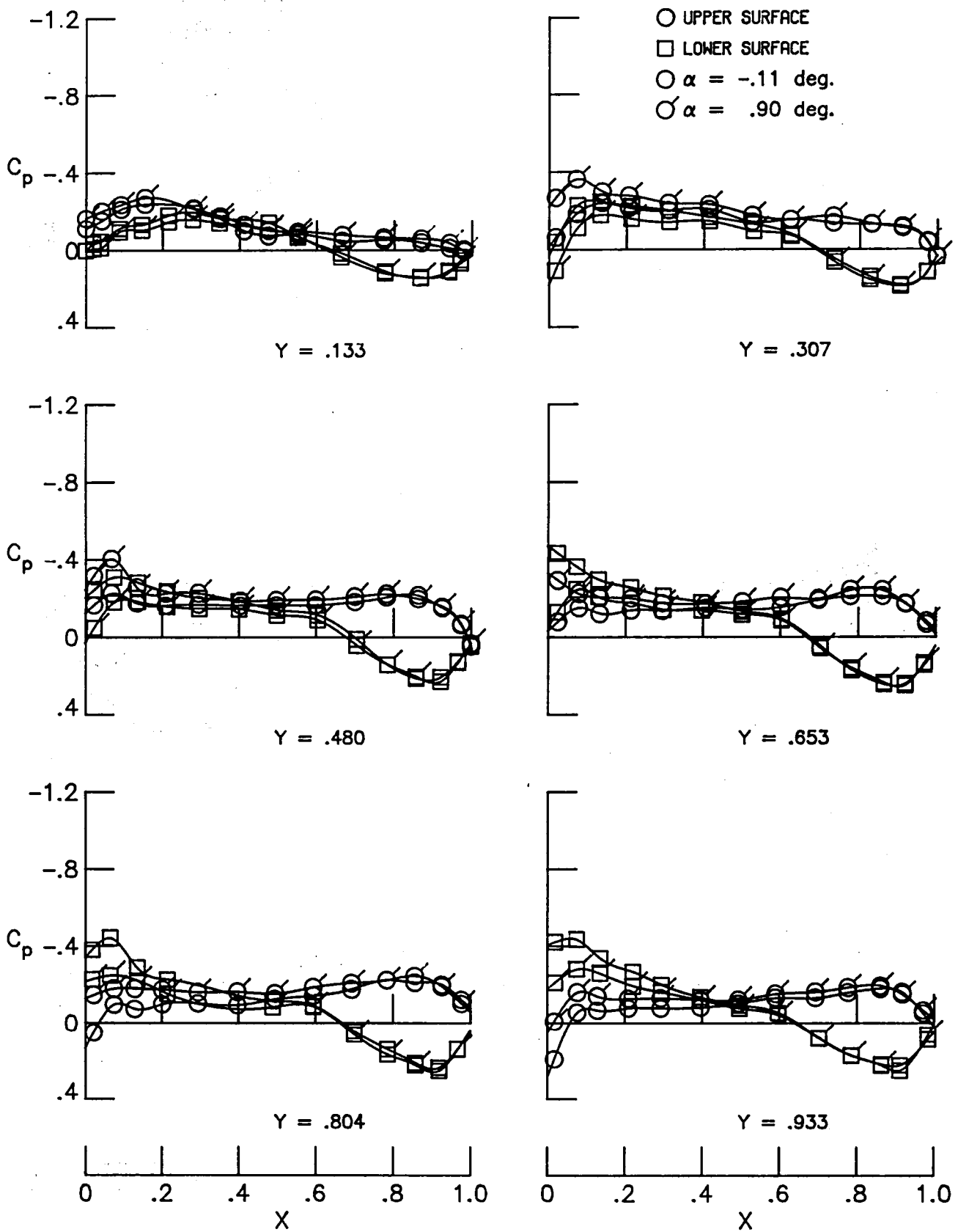
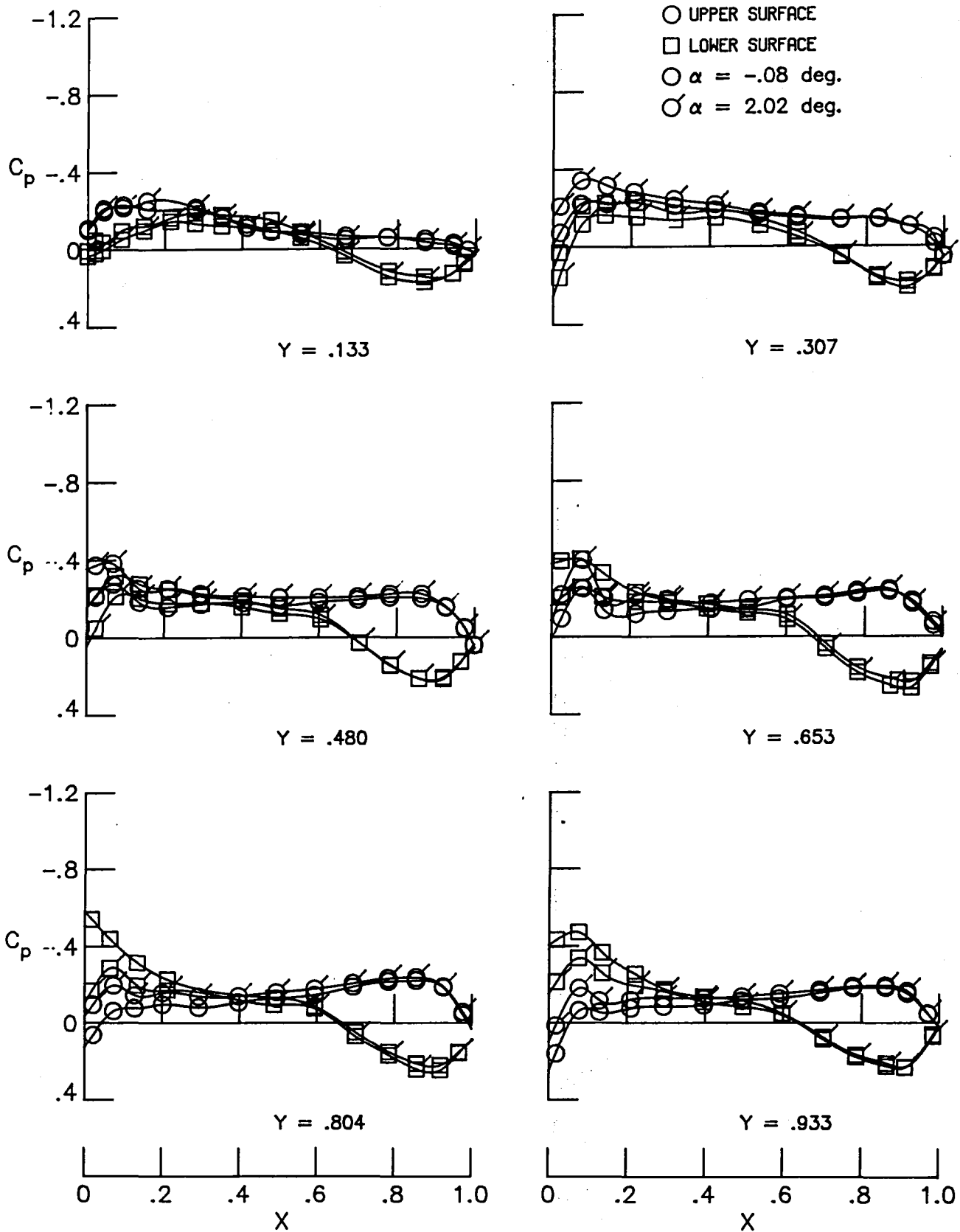


Fig. 2 Bending and torsional components of measured natural vibration modes.



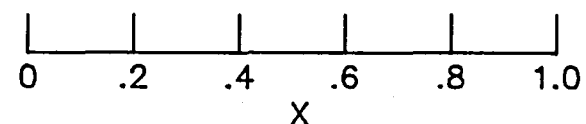
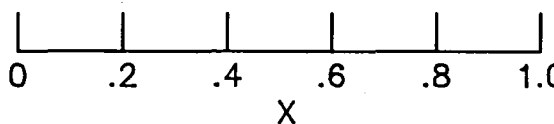
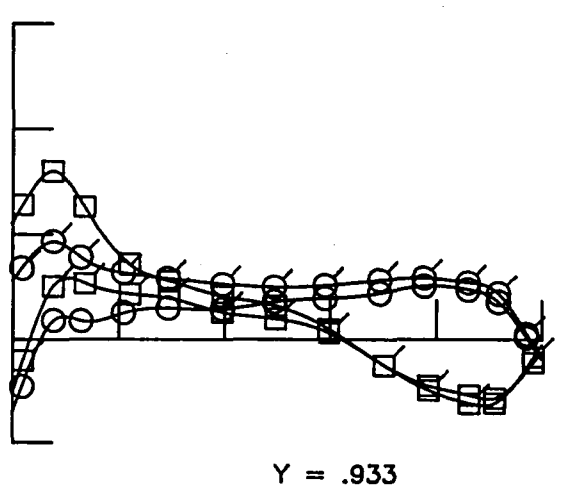
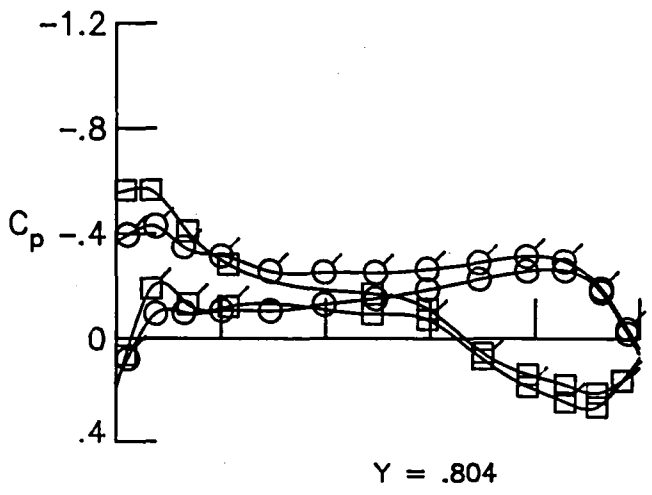
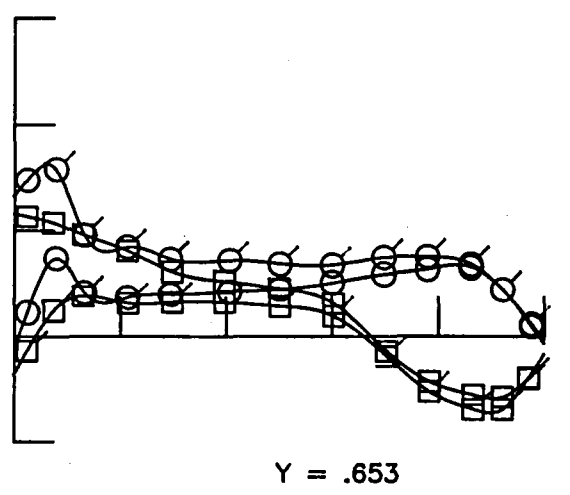
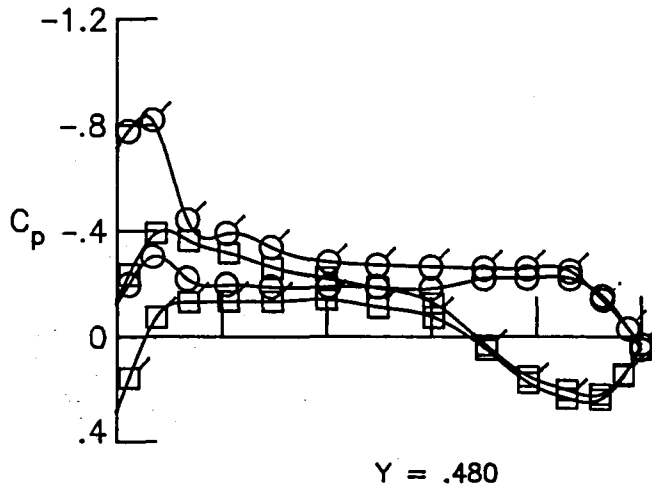
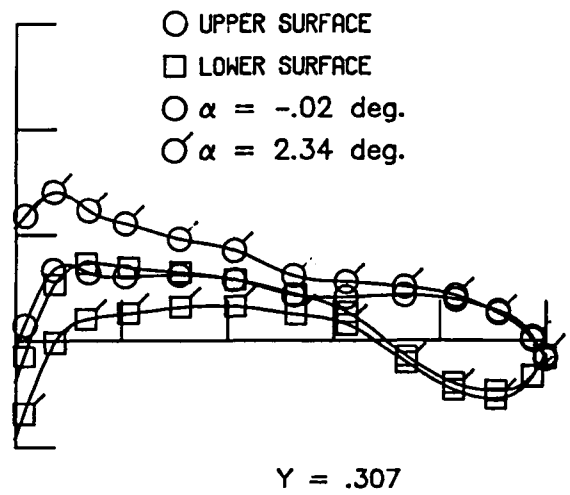
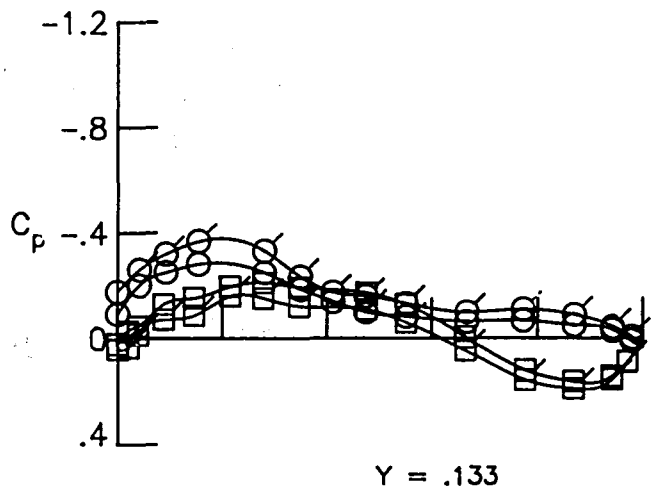
(a) $M = .25$, $q = 5.51$ kPa

Fig. 3 Pressure distributions measured in 8-Foot Transonic Pressure Tunnel.



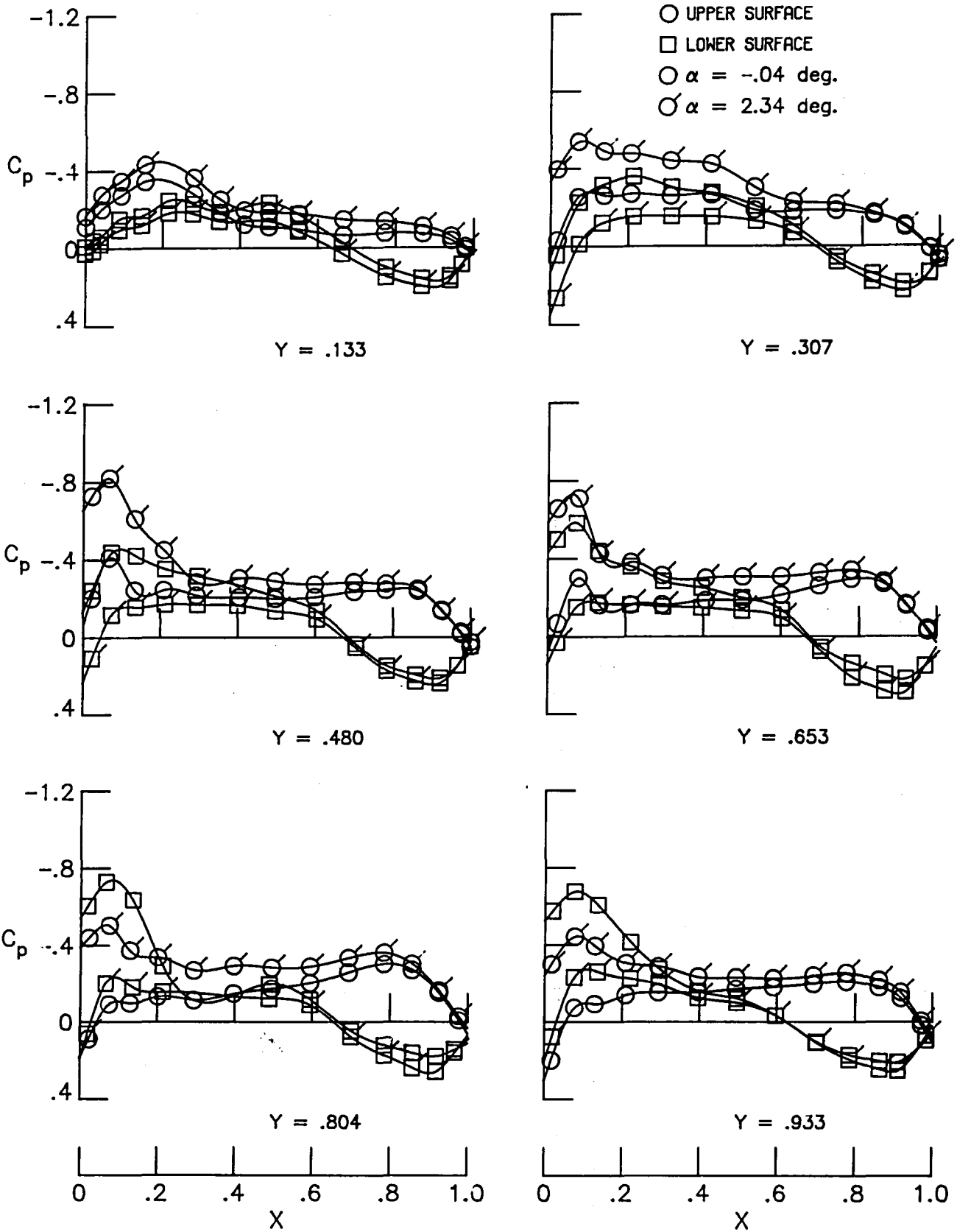
(b) $M = .50$, $q = 15.6$ kPa

Fig. 3 Continued.



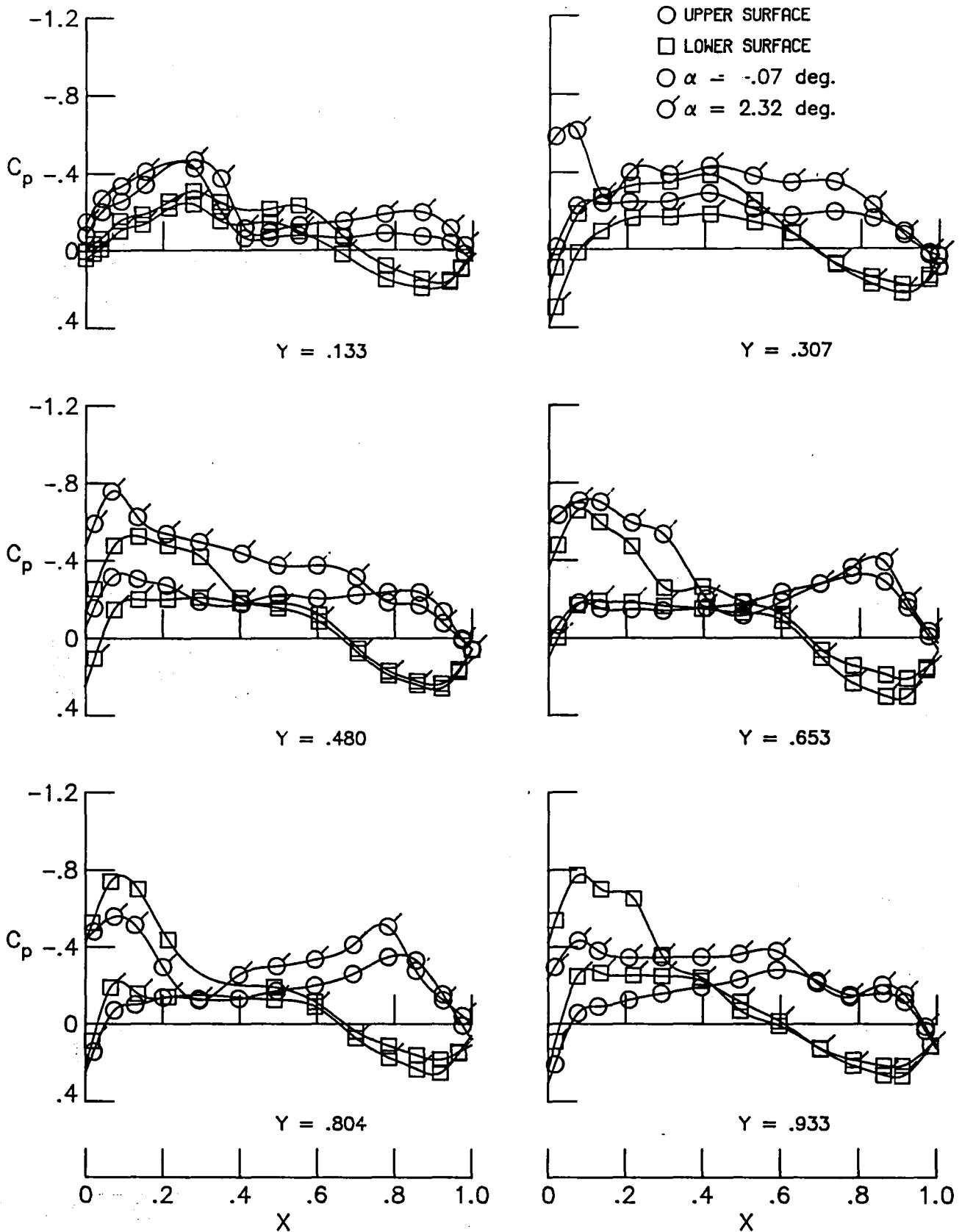
(c) $M = .80$, $q = 31.1$ kPa

Fig. 3 Continued.



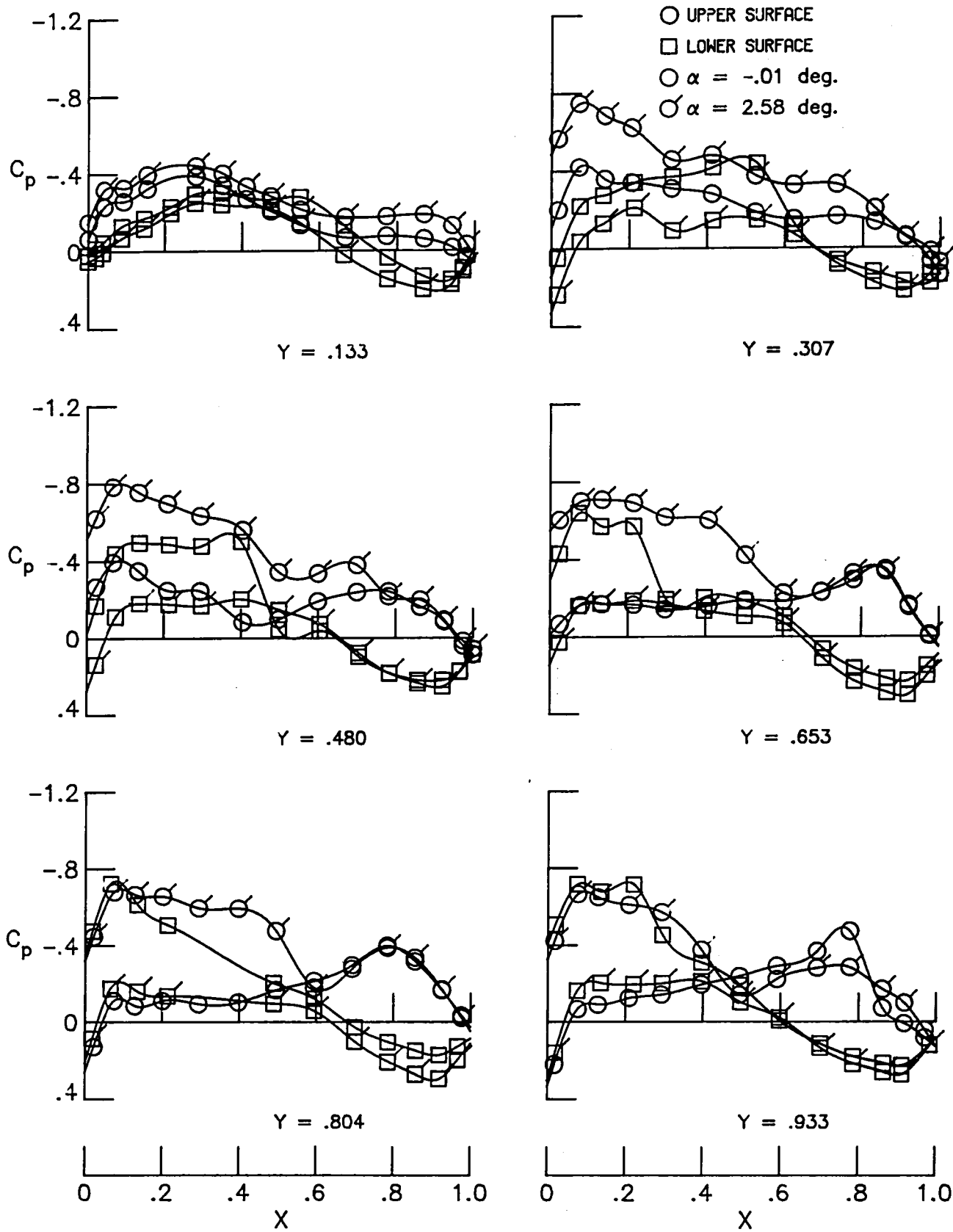
(d) $M = .90$, $q = 31.1$ kPa

Fig. 3 Continued.



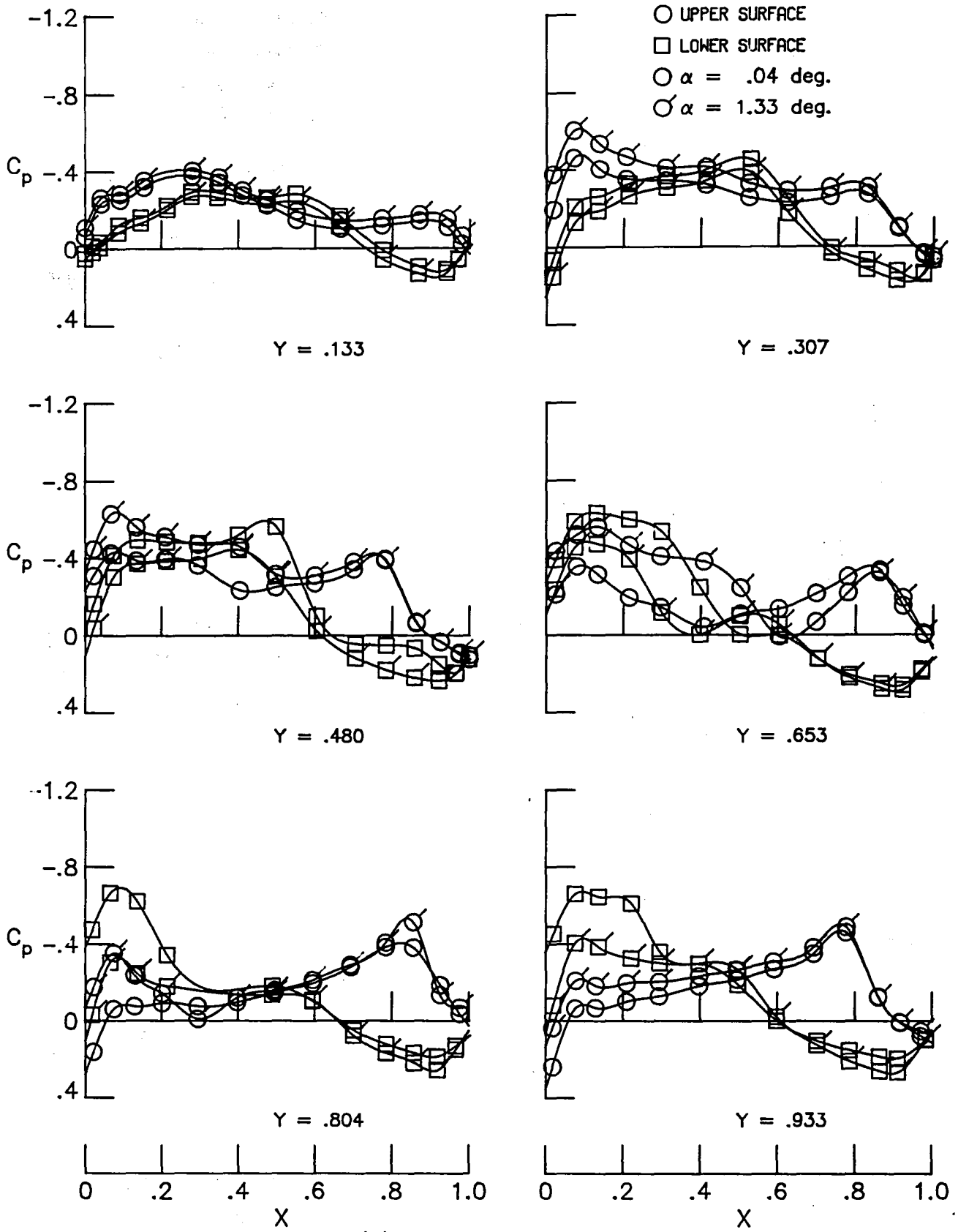
(e) $M = .95$, $q = 28.7$ kPa

Fig. 3 Continued.



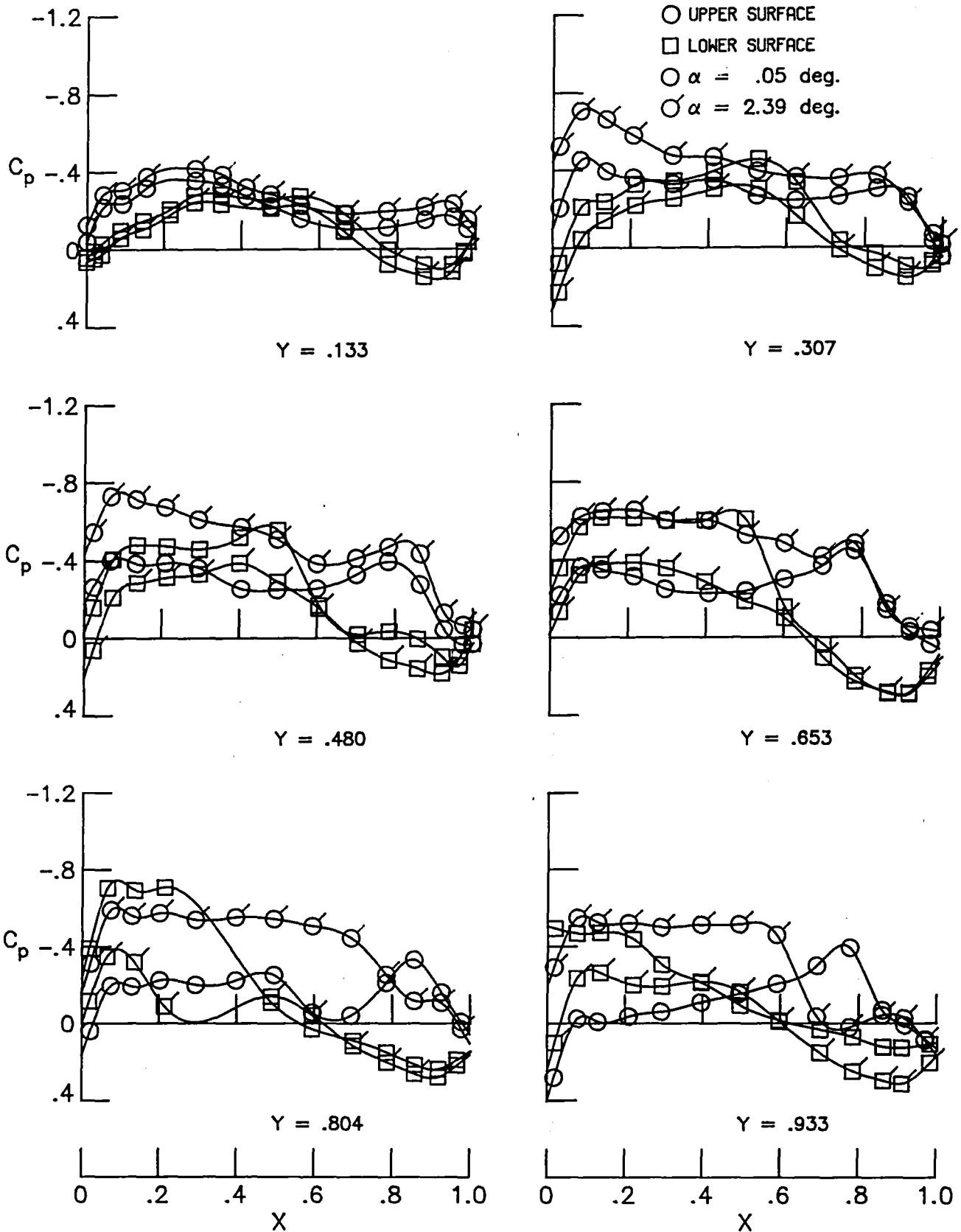
(f) $M = .98$, $q = 28.7$ kPa

Fig. 3 Continued.



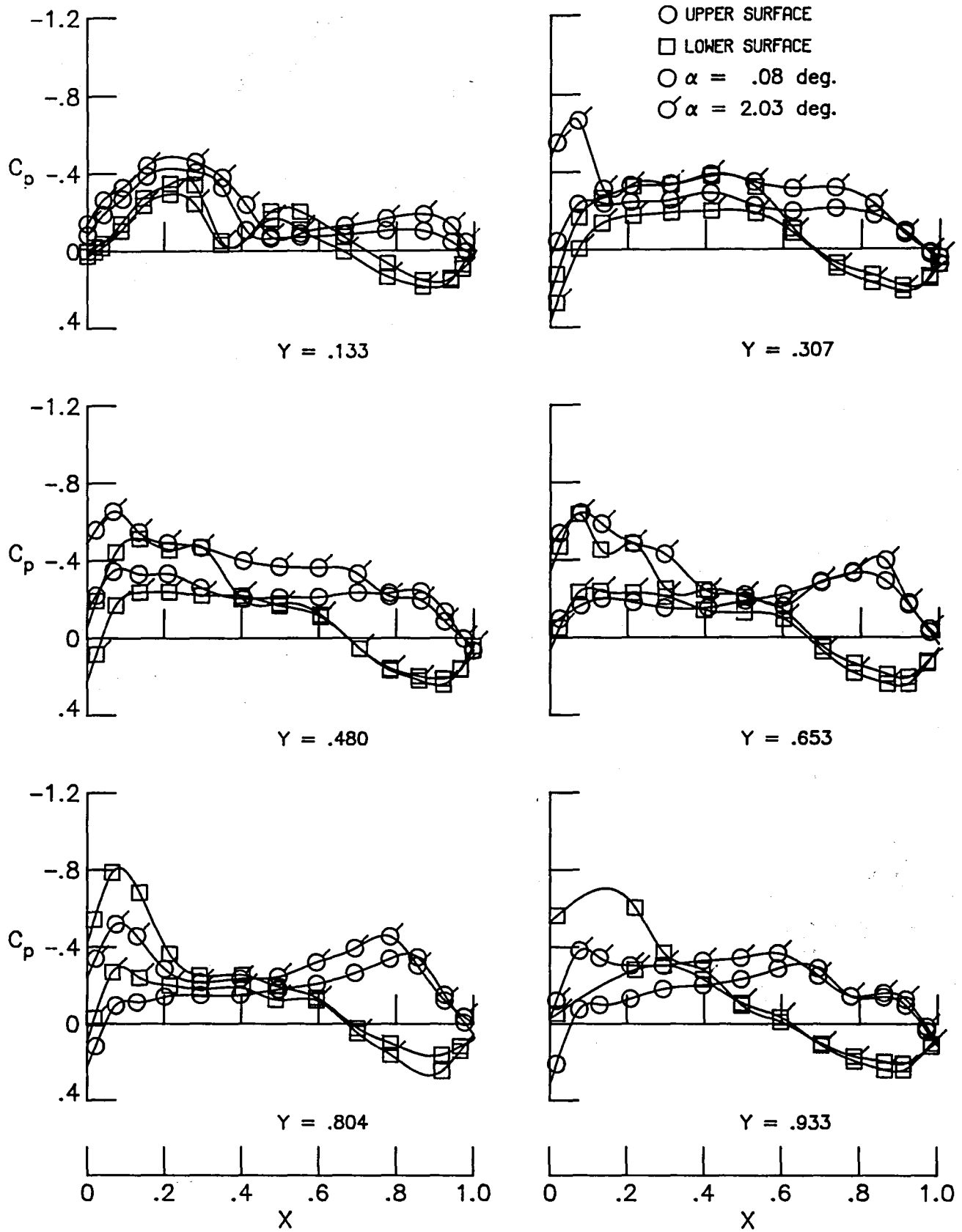
(g) $M = .99$, $q = 28.7$ kPa

Fig. 3 Continued.



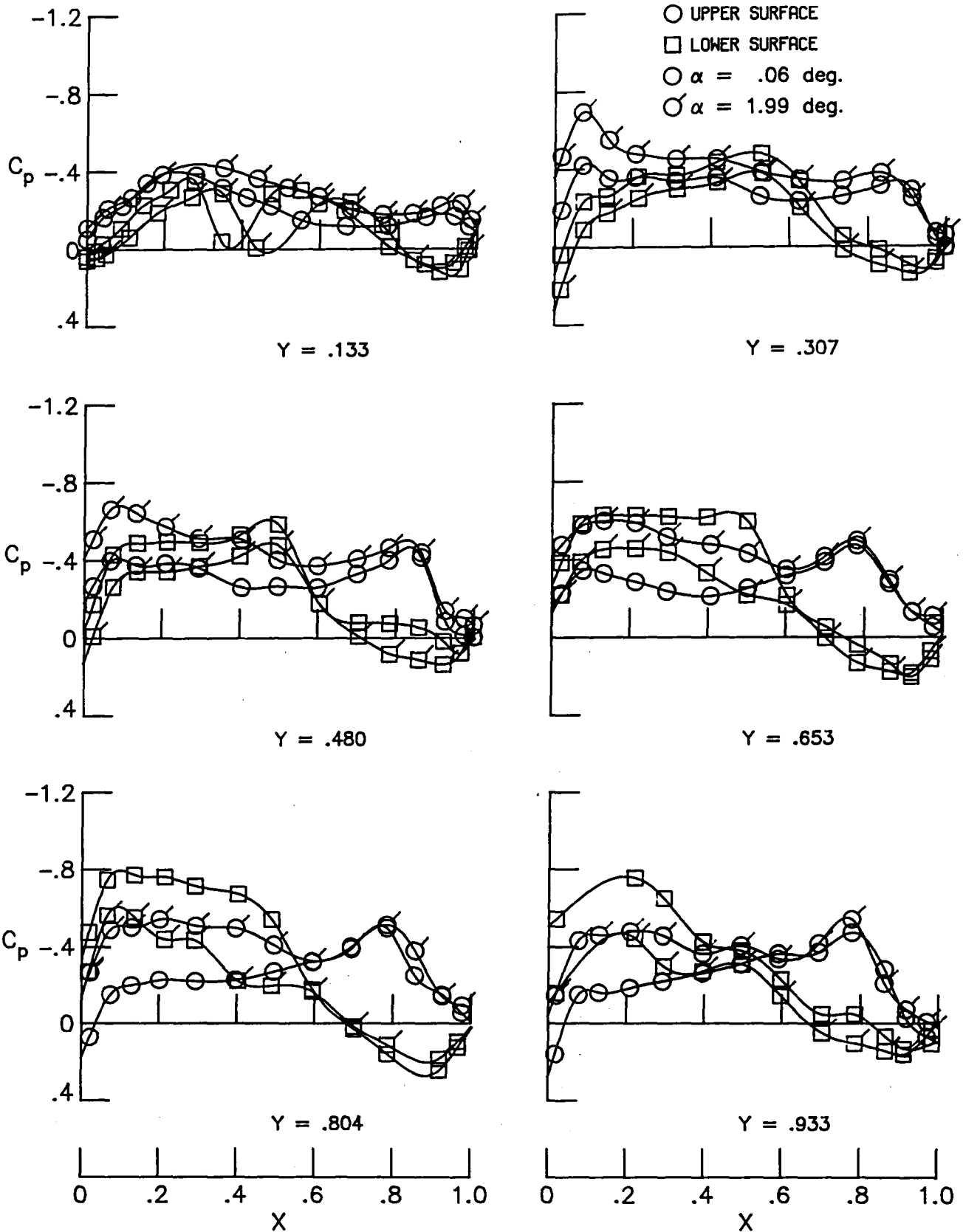
(h) $M = 1.00$, $q = 28.7$ kPa

Fig. 3 Concluded.



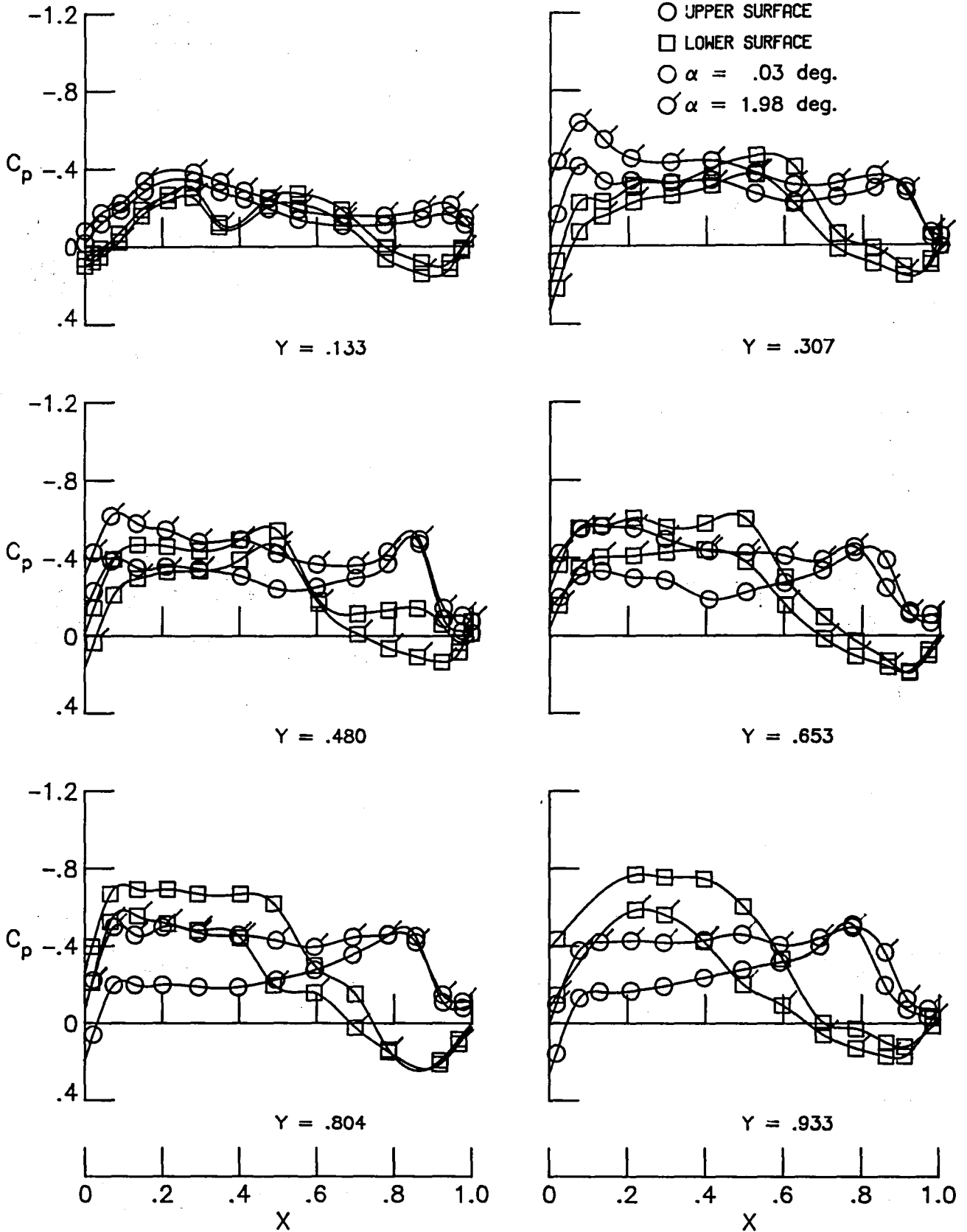
(a) $M = .95$, $q = 35.4$ kPa

Fig. 4 Pressure distributions measured in 16-Foot Transonic Tunnel.



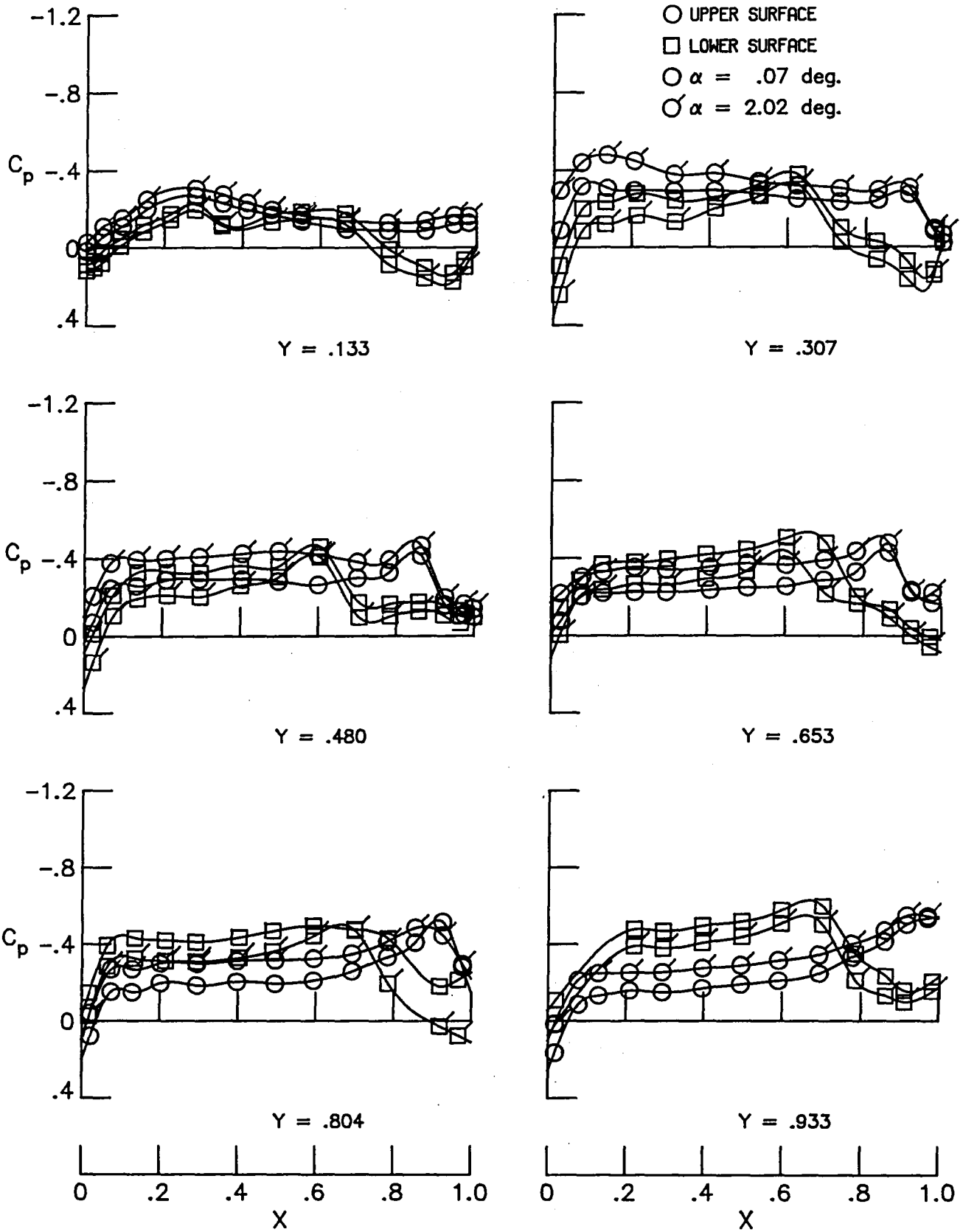
(b) $M = .99$, $q = 36.7$ kPa

Fig. 4 Continued.



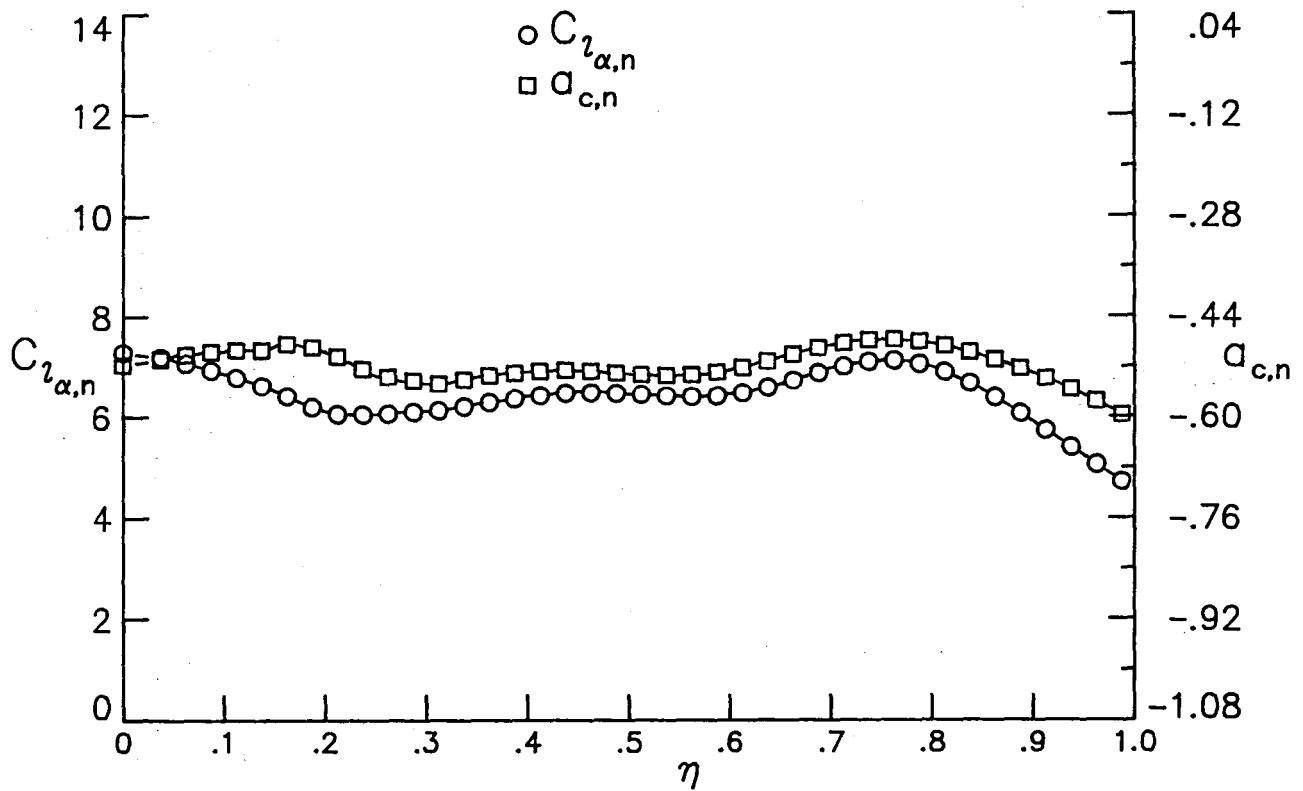
(c) $M = 1.02$, $q = 37.6$ kPa

Fig. 4 Continued.

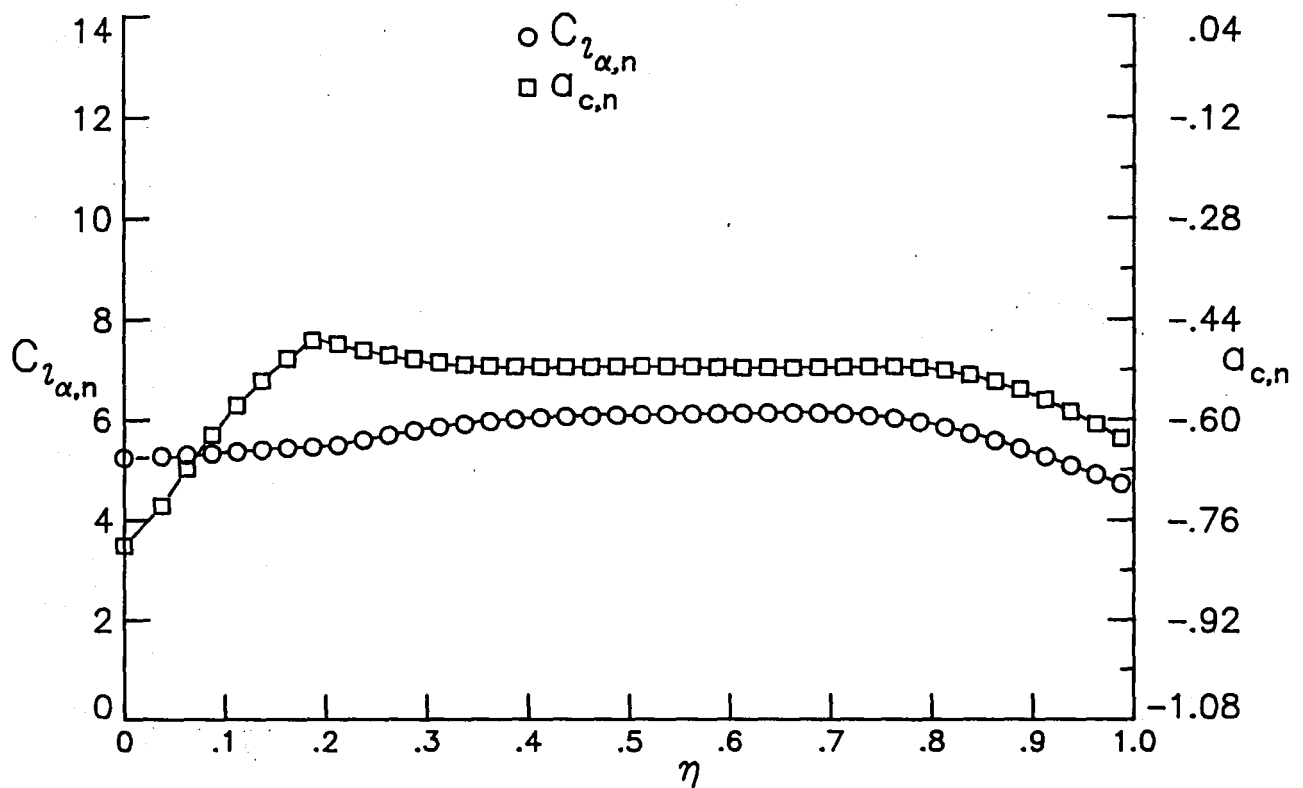


(d) $M = 1.20$, $q = 41.6$ kPa

Fig. 4 Concluded.

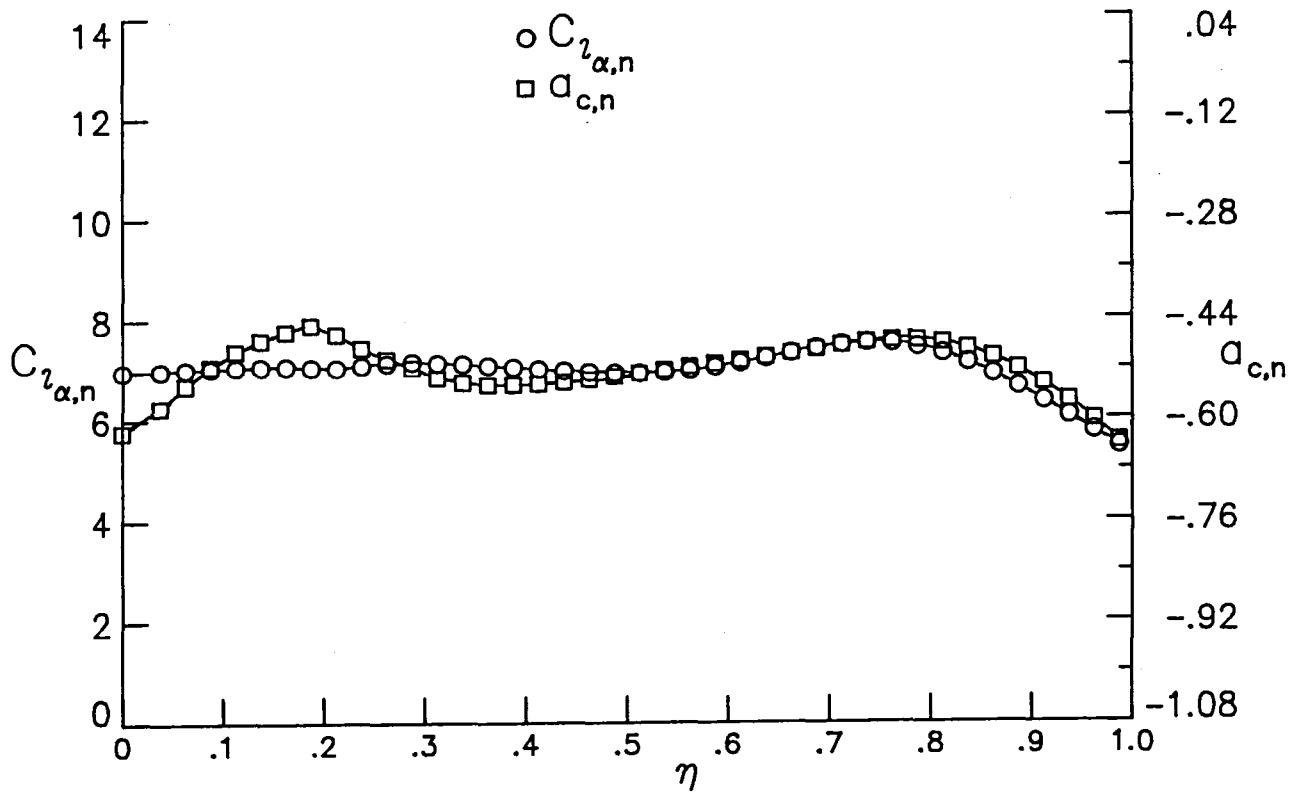


(a) $M = .25$, $q = 5.51$ kPa

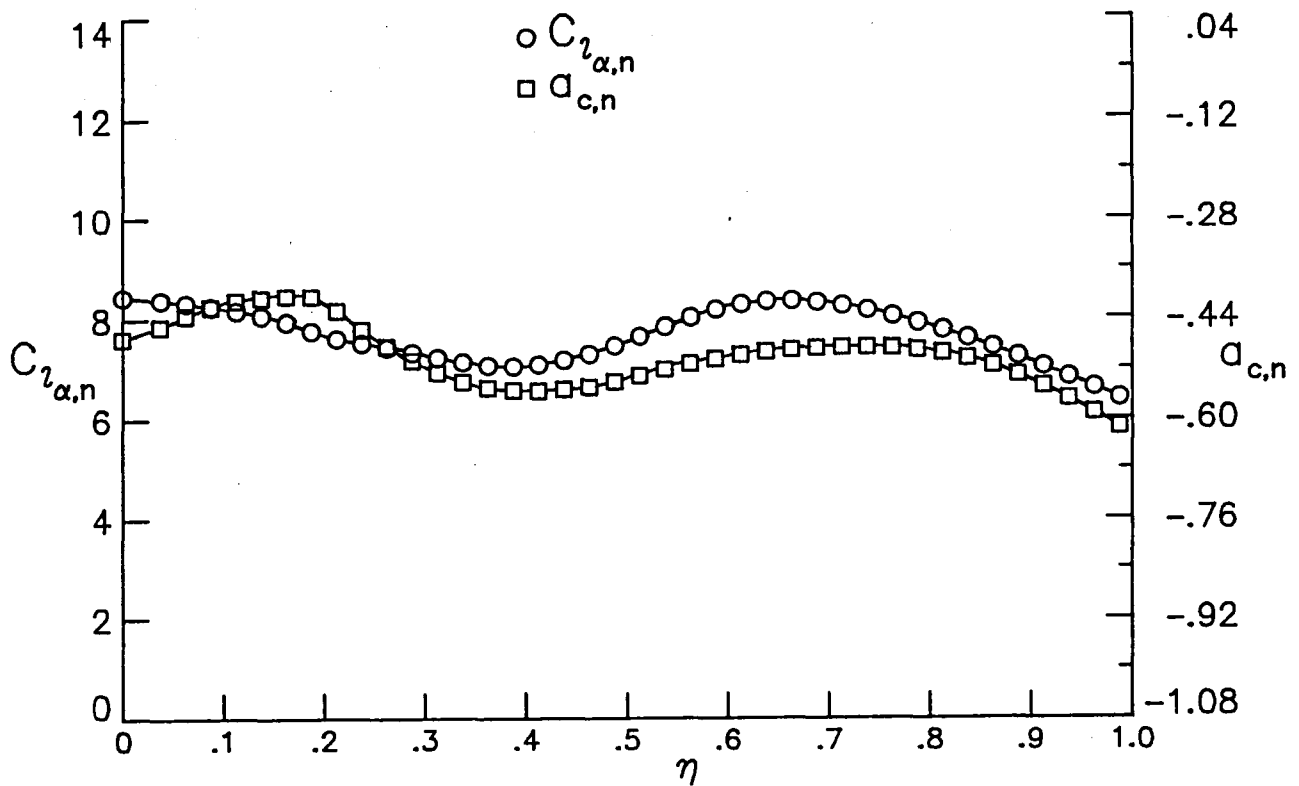


(b) $M = .50$, $q = 15.6$ kPa

Fig. 5 Aerodynamic parameters for flutter analysis from 8-foot tunnel data.

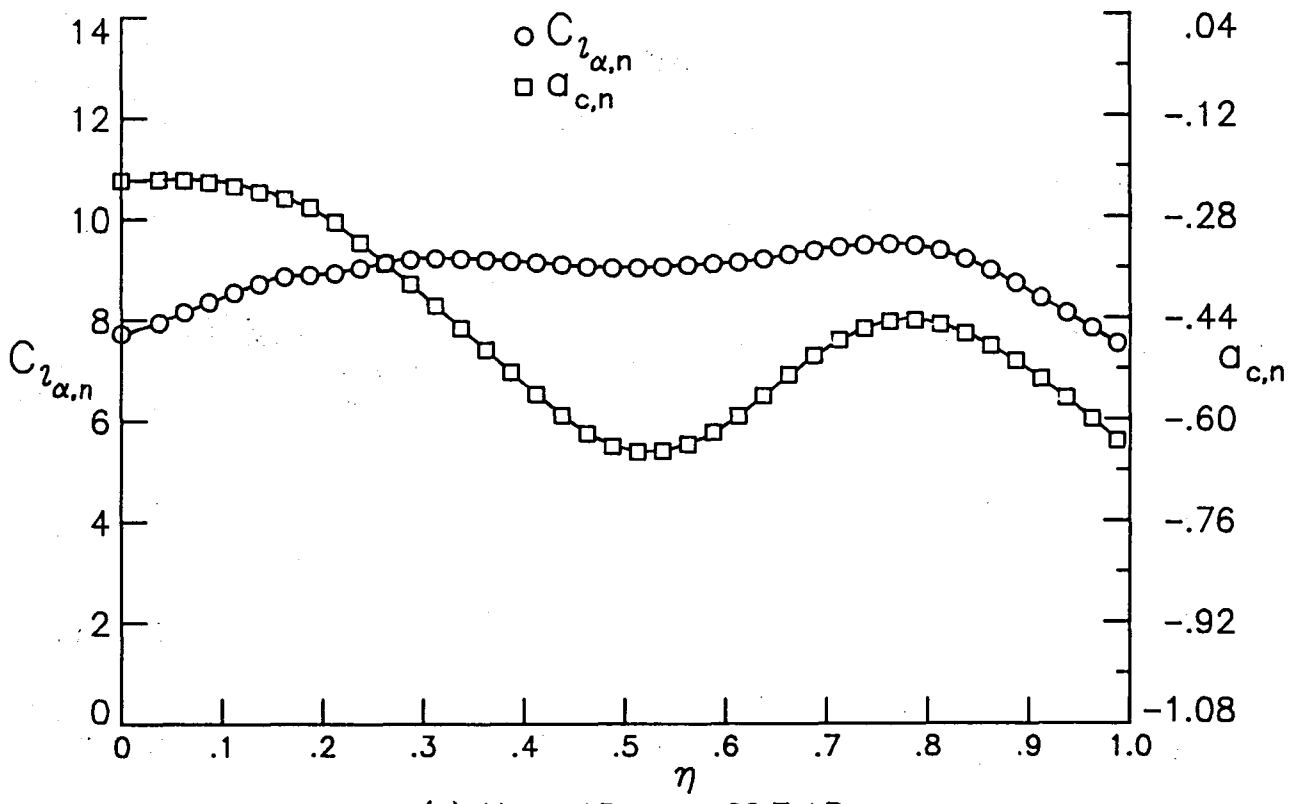


(c) $M = .80, q = 31.1$ kPa

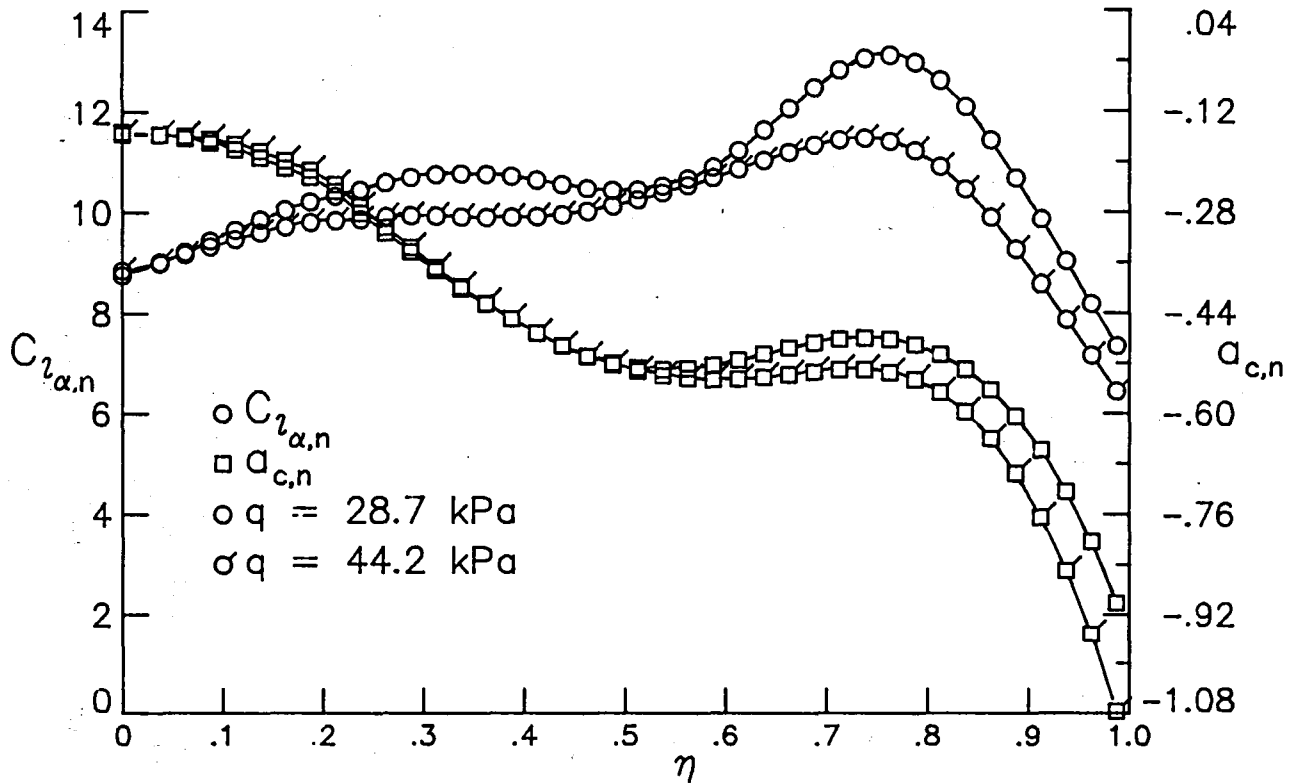


(d) $M = .90, q = 31.1$ kPa

Fig. 5 Continued.

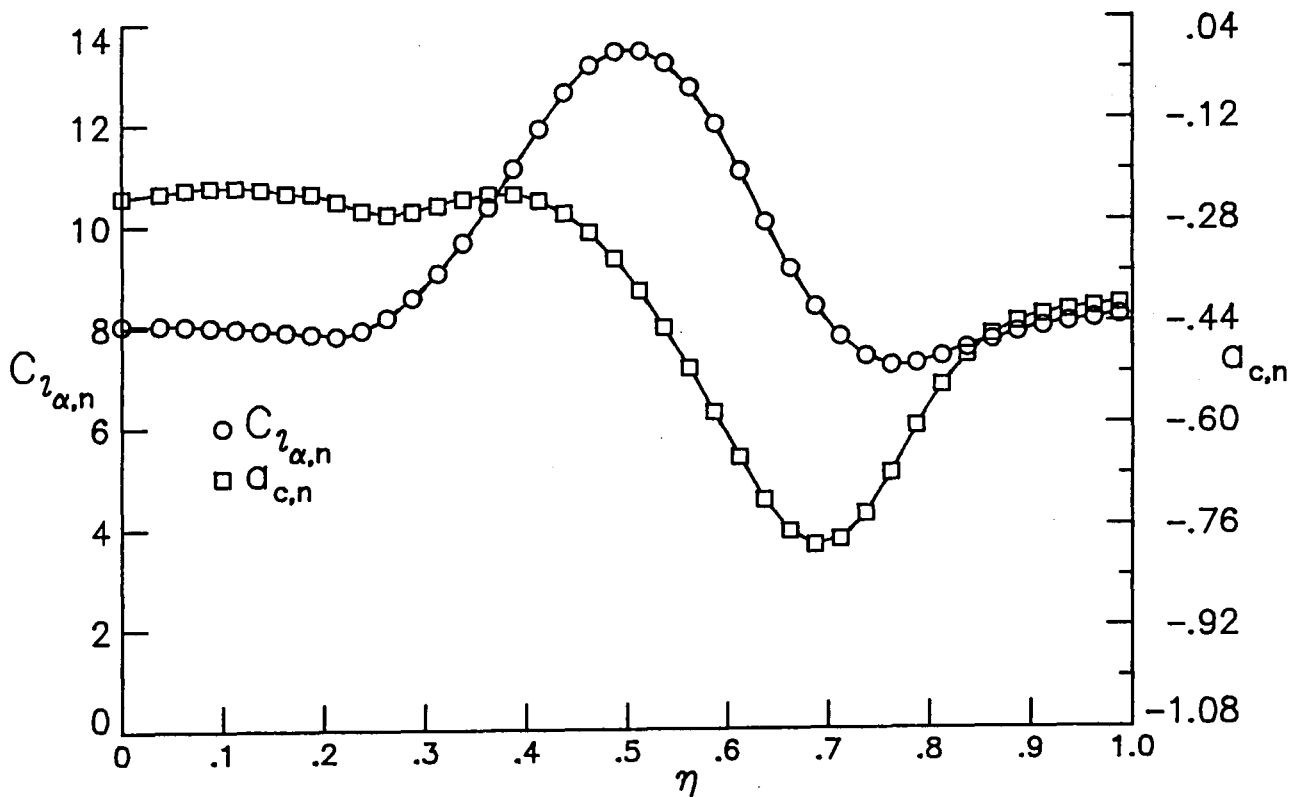


(e) $M = .95, q = 28.7$ kPa

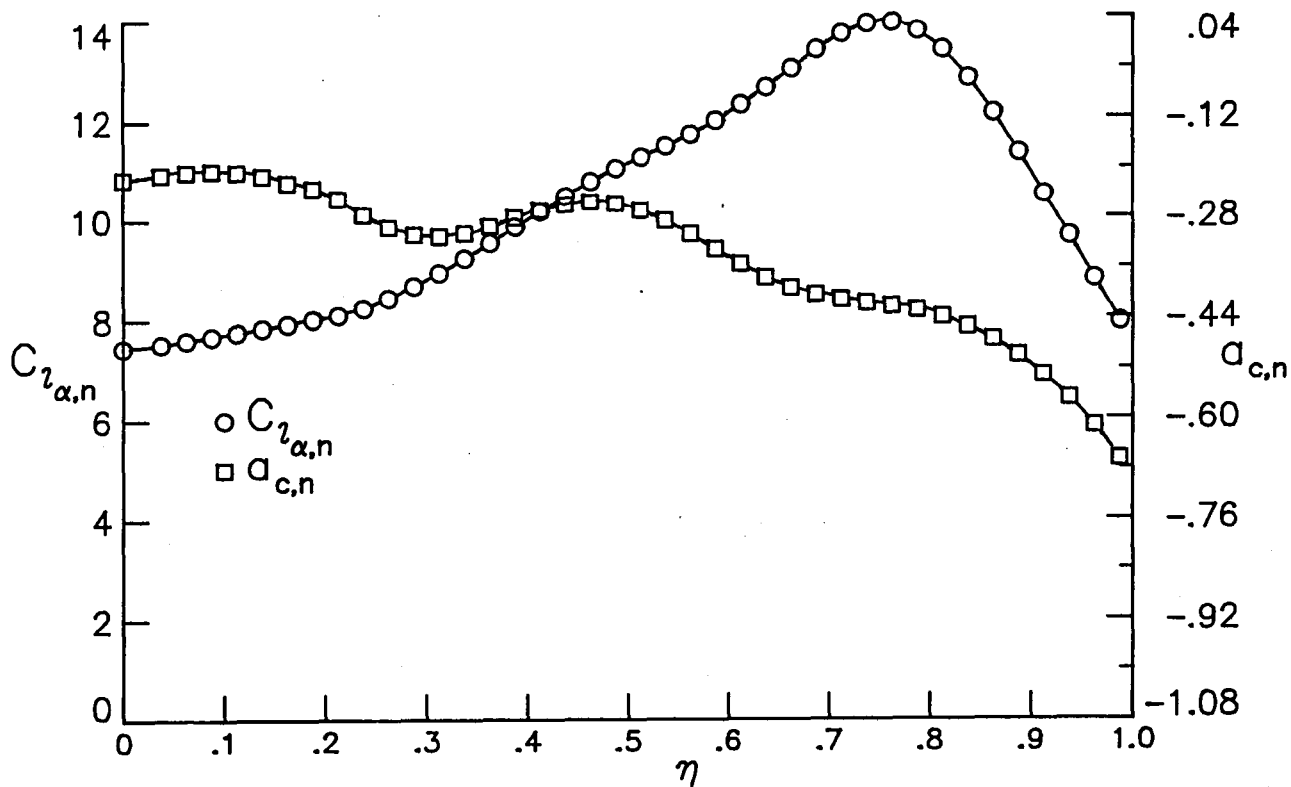


(f) $M = .98$

Fig. 5 Continued.

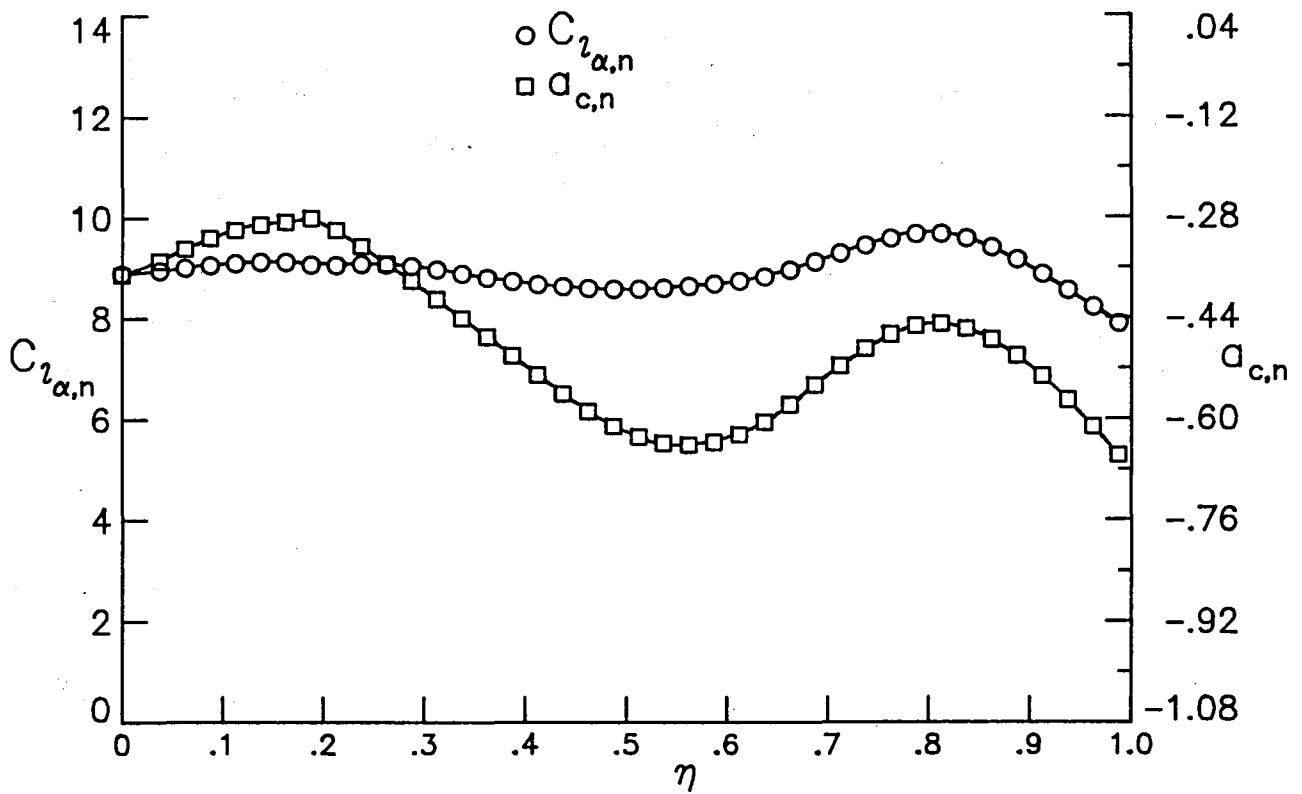


(g) $M = .99, q = 28.7$ kPa

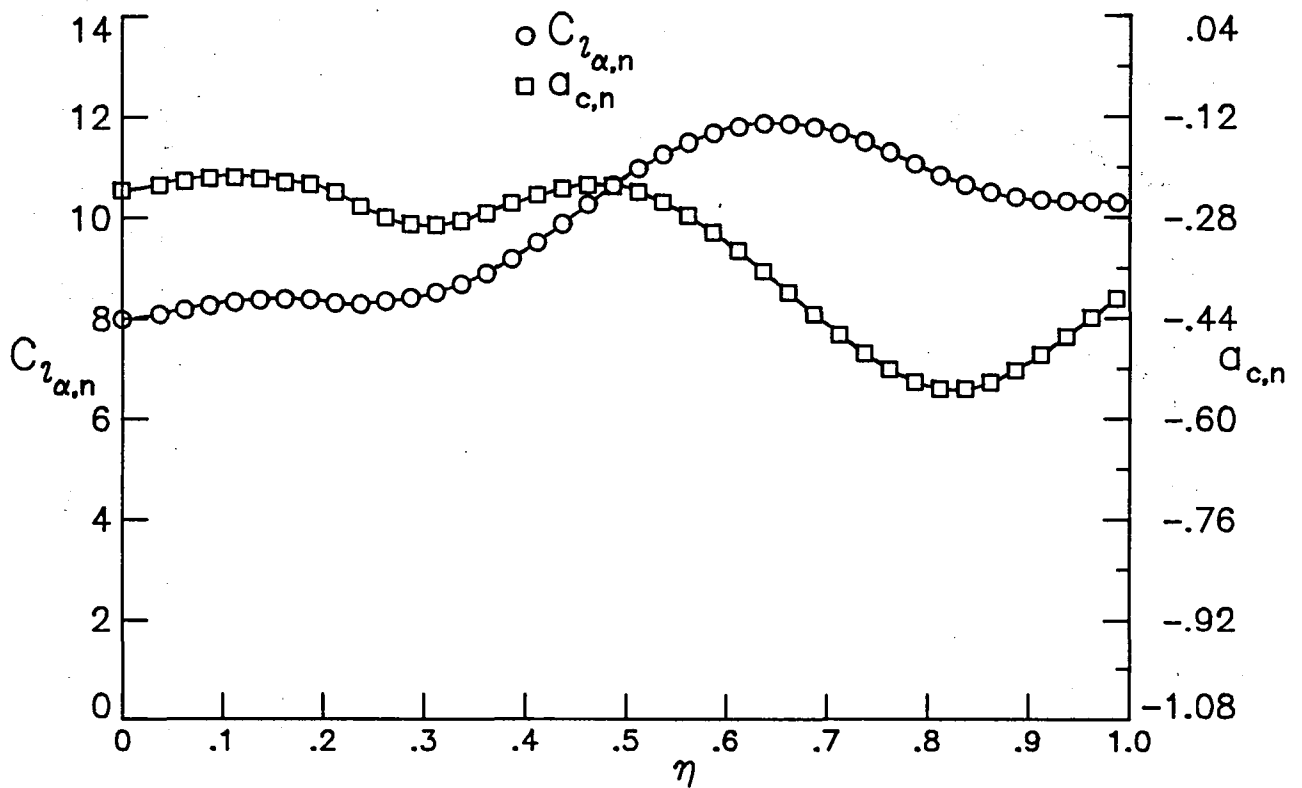


(h) $M = 1.00, q = 28.7$ kPa

Fig. 5 Concluded.

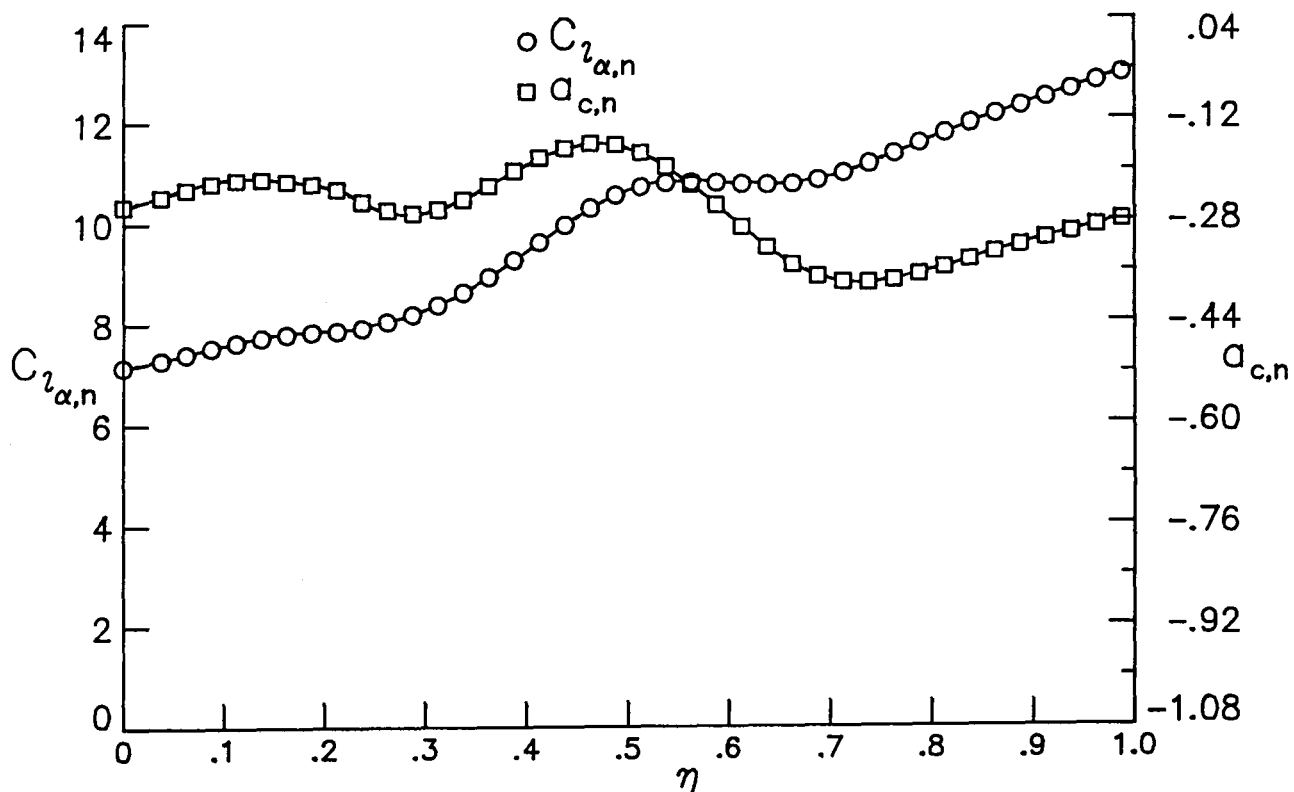


(a) $M = .95$, $q = 35.4$ kPa

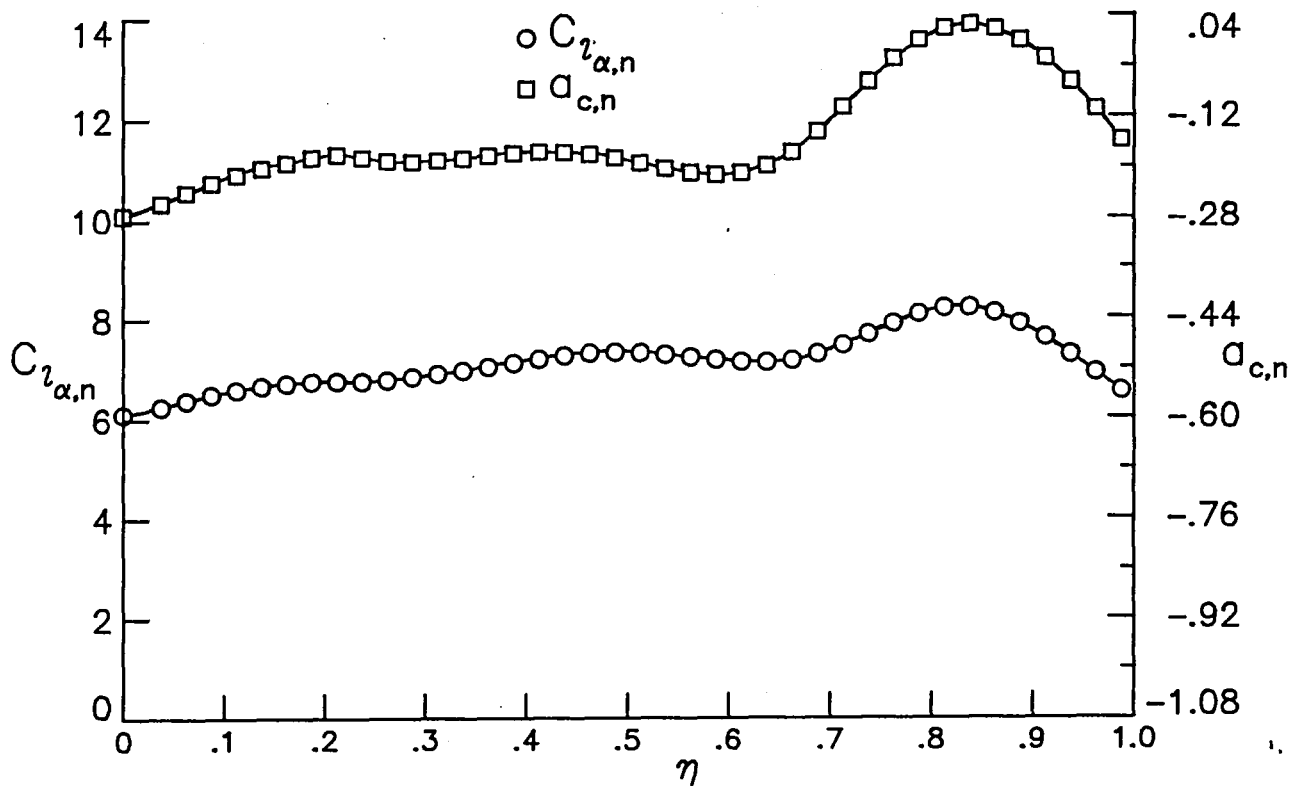


(b) $M = .99$, $q = 36.7$ kPa

Fig. 6 Aerodynamic parameters for flutter analysis from 16-foot tunnel data.



(c) $M = 1.02$, $q = 37.6$ kPa



(d) $M = 1.20$, $q = 41.6$ kPa

Fig. 6 Concluded.

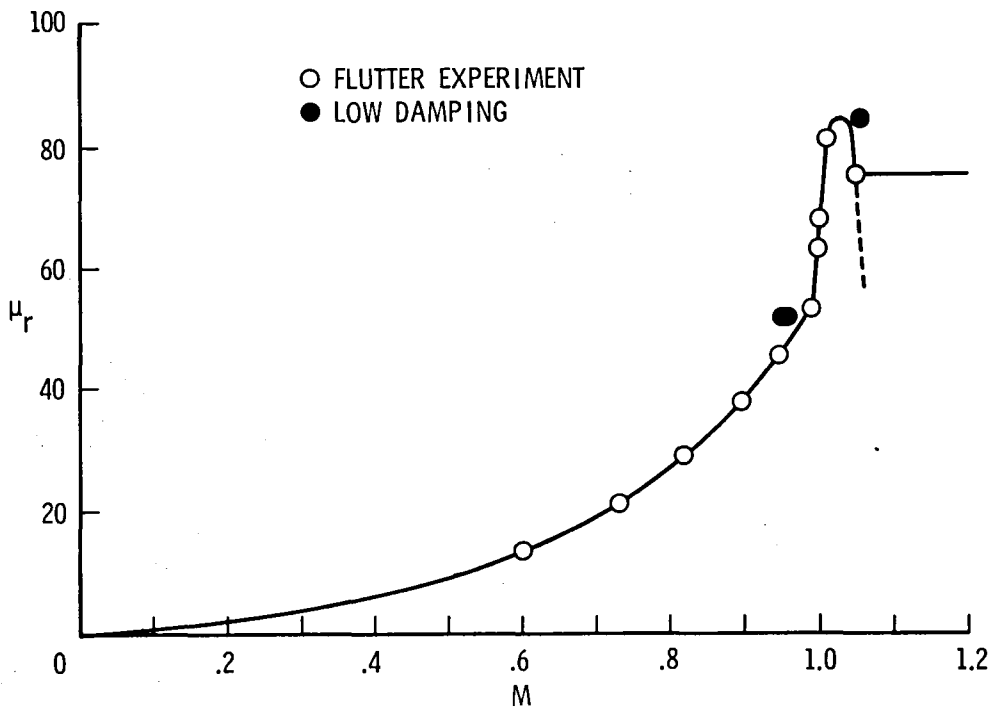


Fig. 7 Mass ratios for flutter experiments.

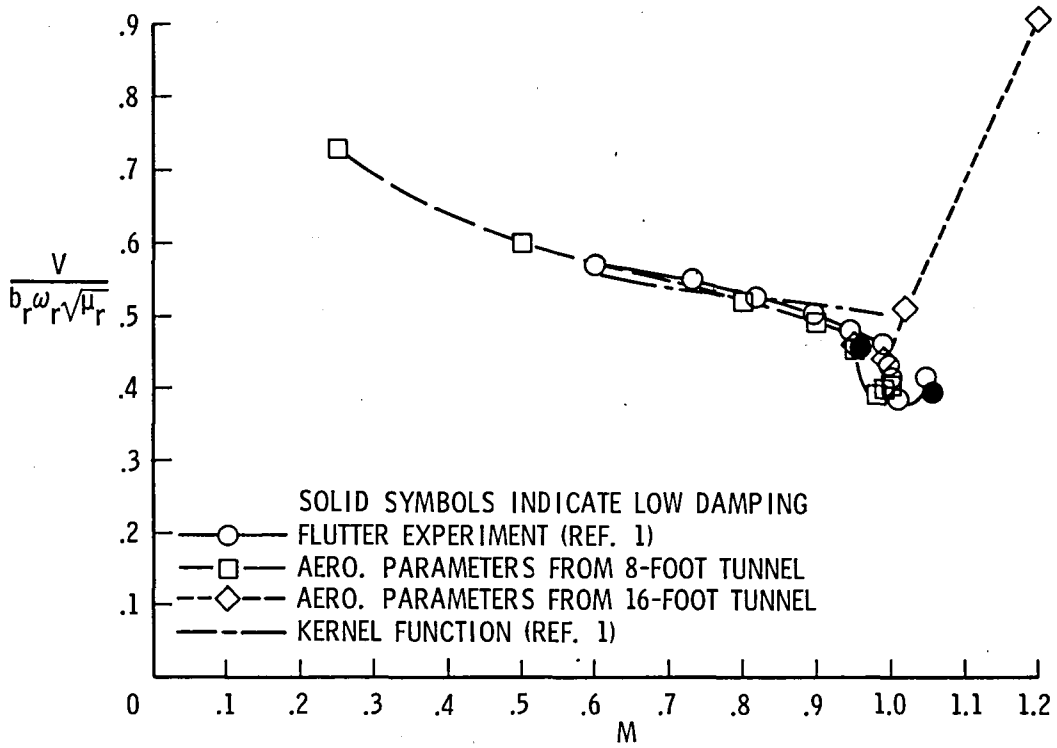


Fig. 8 Comparison of calculated and measured flutter speeds.

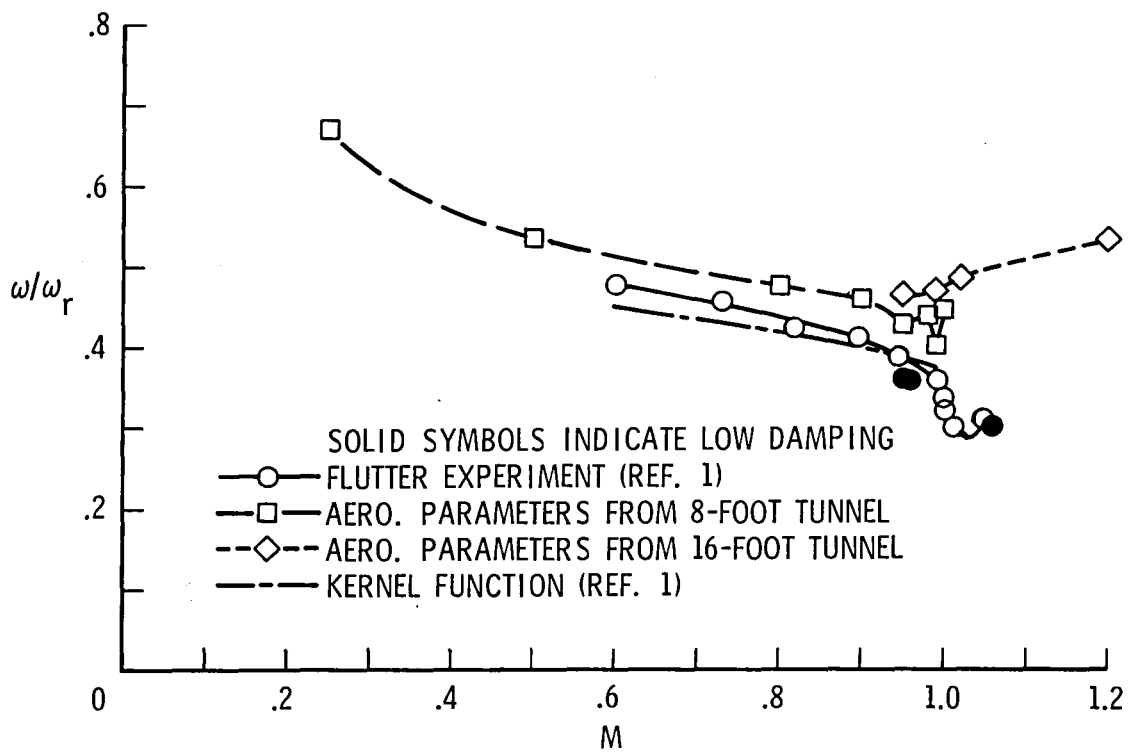


Fig. 9 Comparison of calculated and measured flutter frequencies.

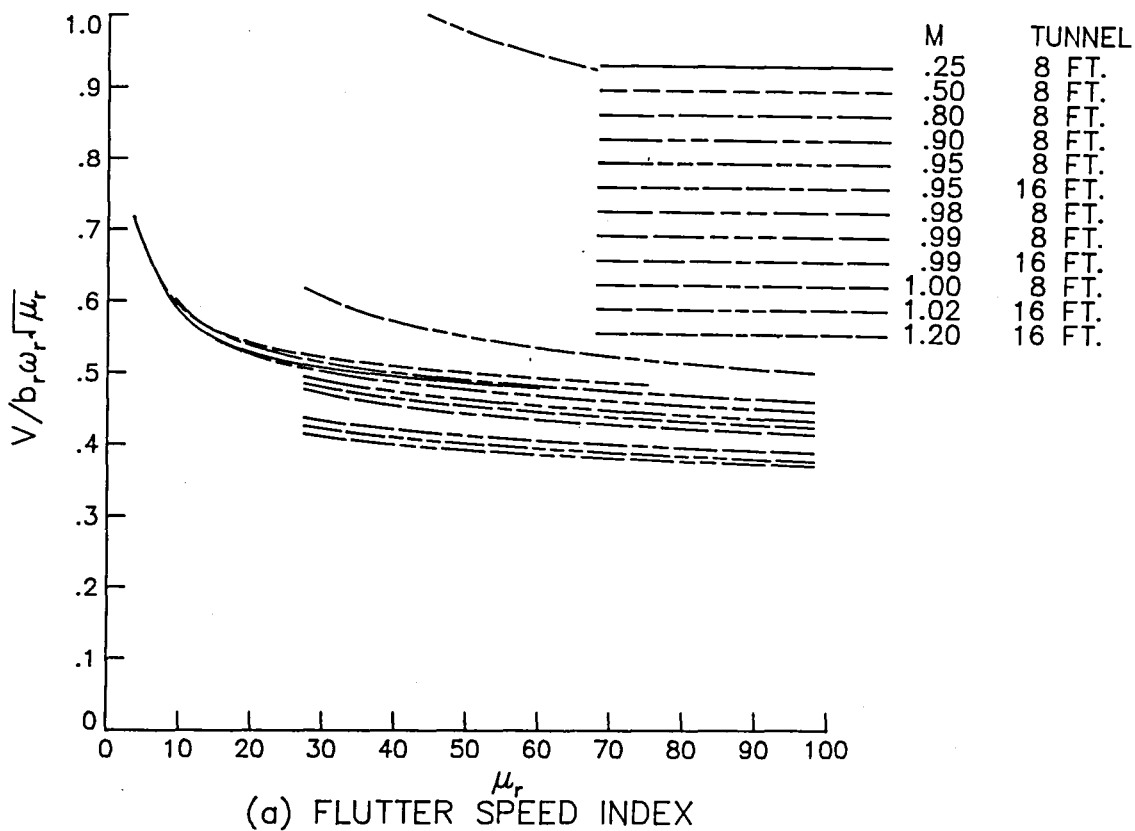
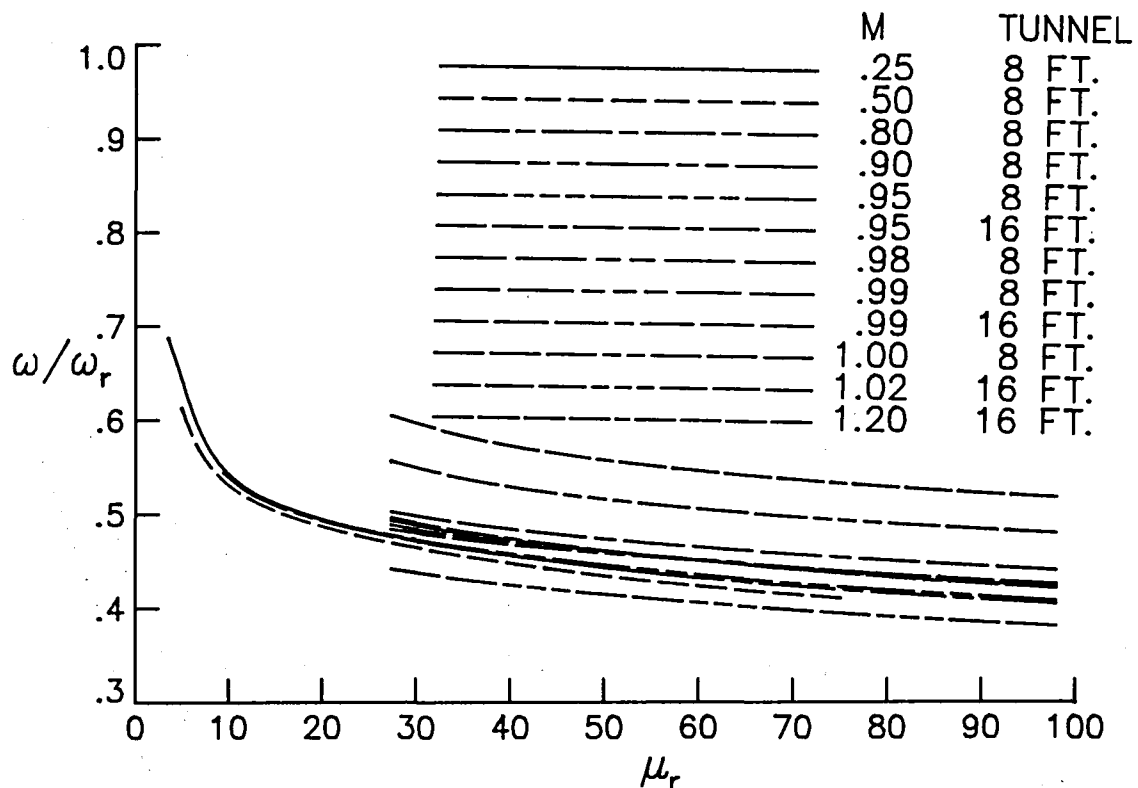
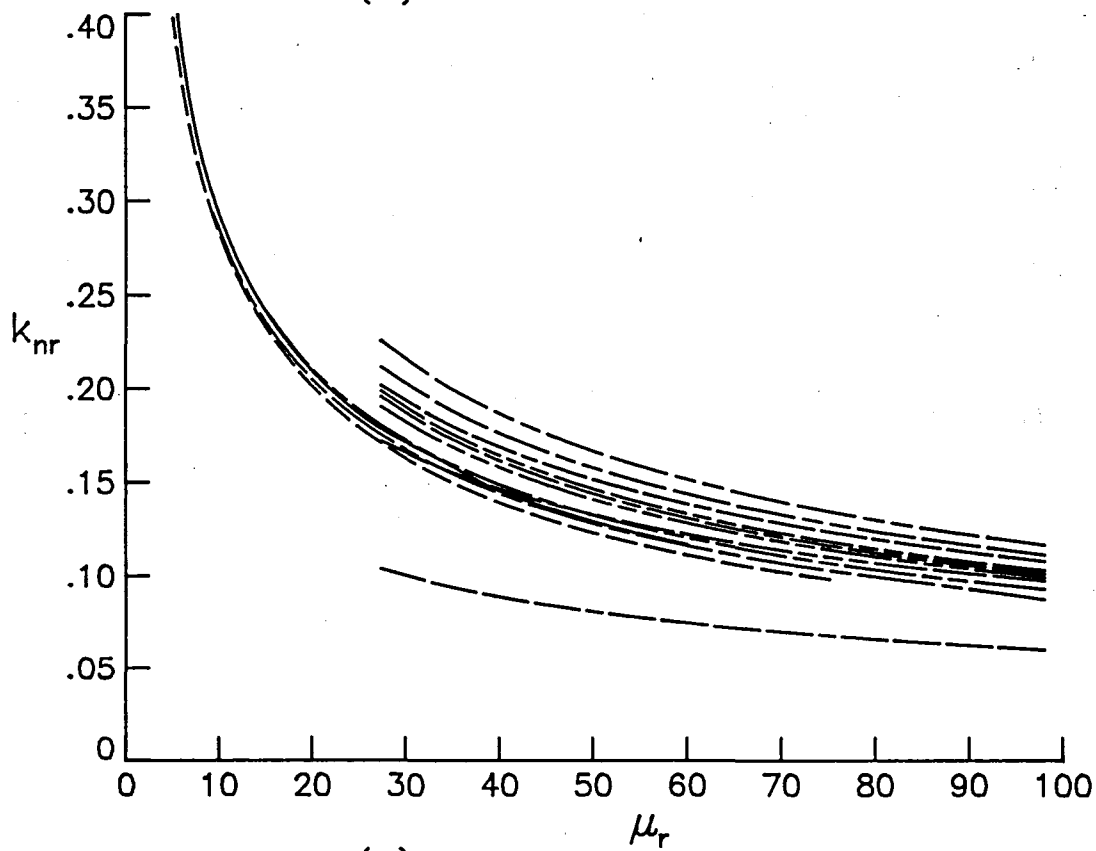


Fig. 10 Variation of calculated flutter characteristics with mass ratio.



(b) FLUTTER FREQUENCY



(c) REDUCED FREQUENCY

Fig. 10 Concluded.

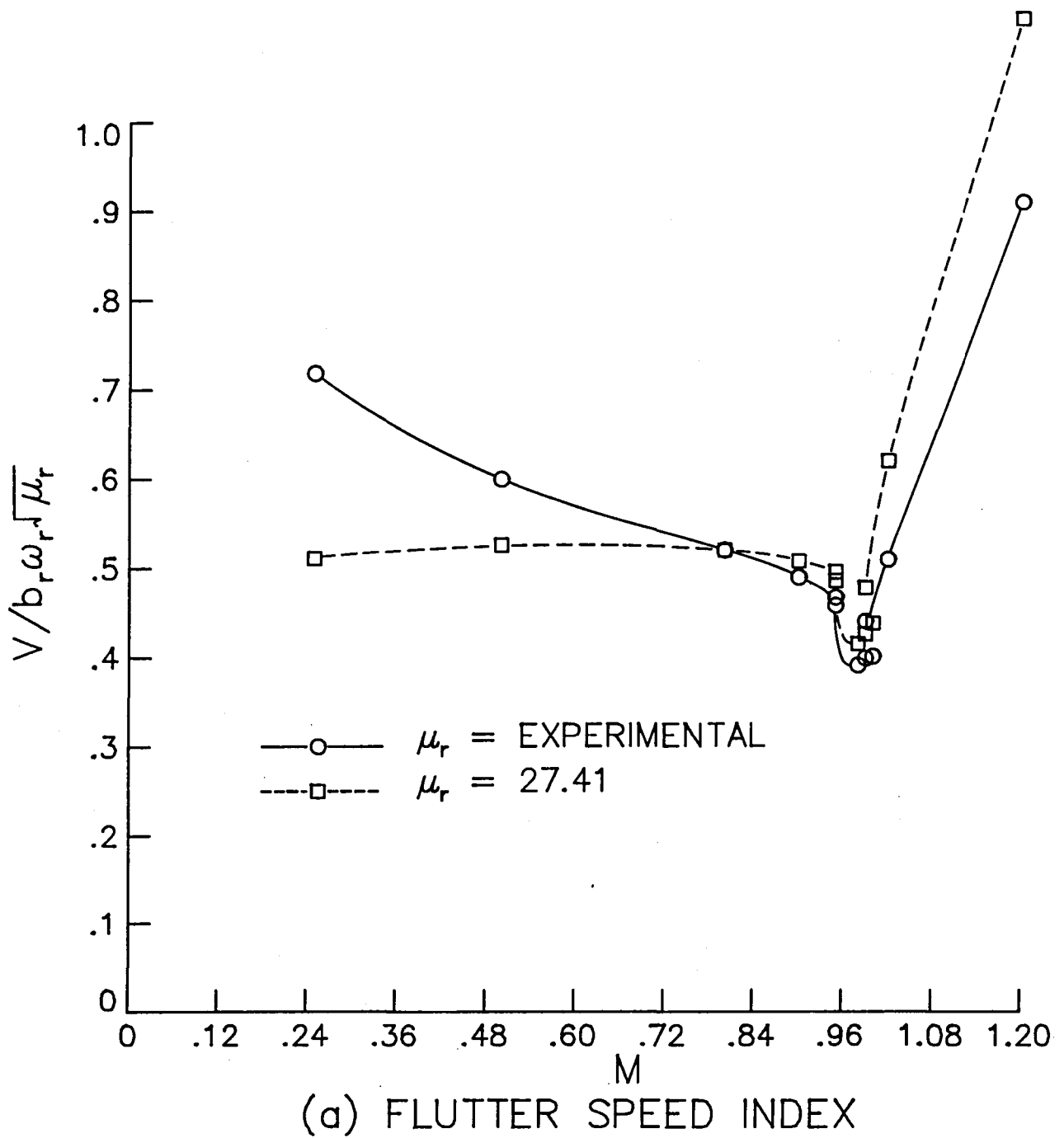
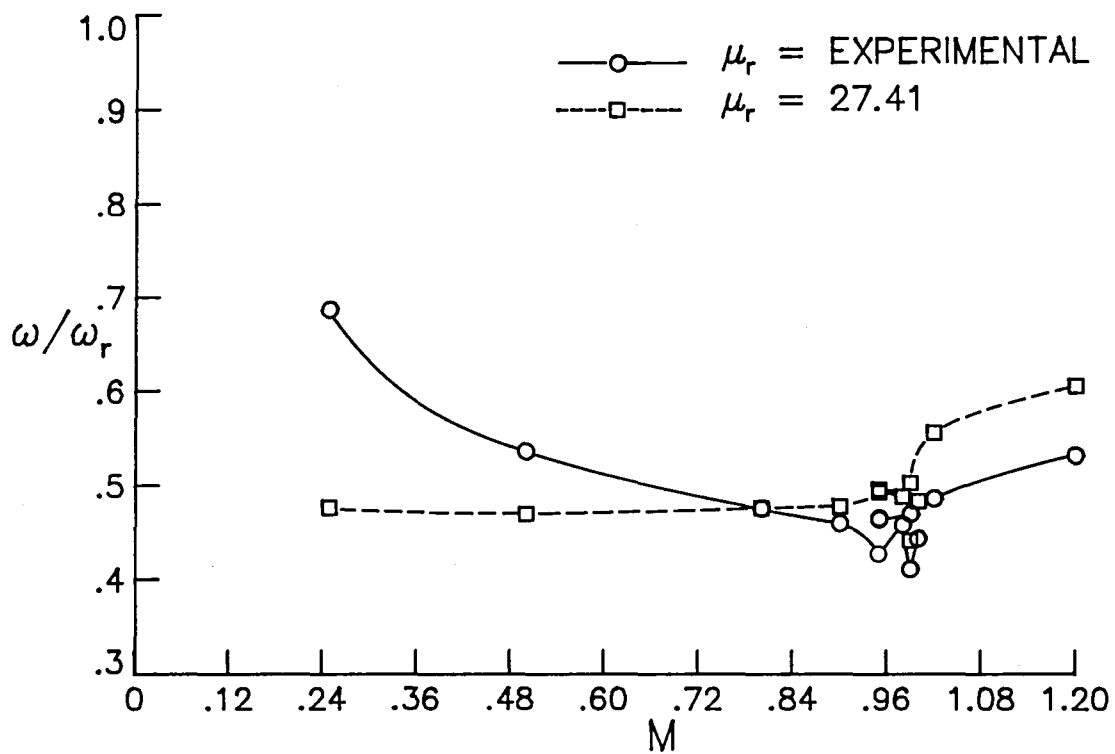
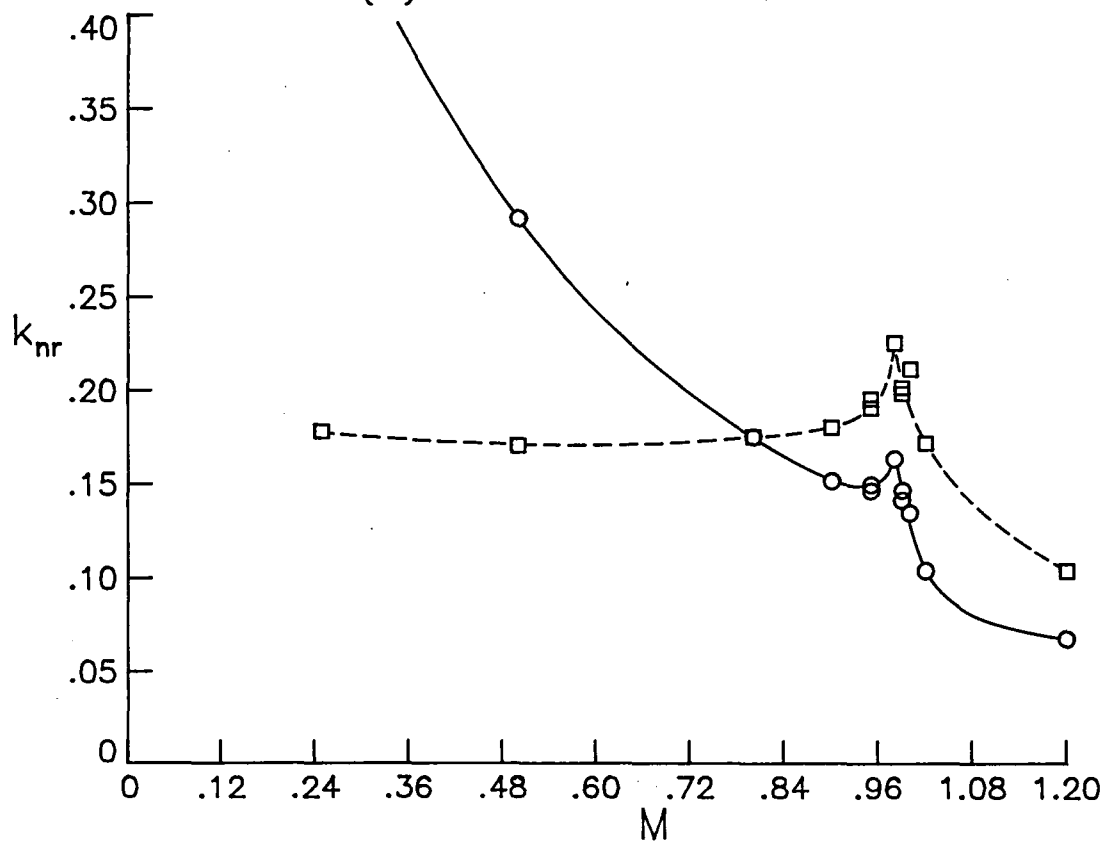


Fig. 11 Comparison of calculated flutter characteristics for constant and varying mass ratio.



(b) FLUTTER FREQUENCY



(c) REDUCED FREQUENCY

Fig. 11 Concluded.

1. Report No. NASA TM-83126		2. Government Accession No.		3. Recipient's Catalog No.	
4. Title and Subtitle PREDICTION OF TRANSONIC FLUTTER FOR A SUPERCRITICAL WING BY MODIFIED STRIP ANALYSIS AND COMPARISON WITH EXPERIMENT				5. Report Date May 1981	
				6. Performing Organization Code 505-33-53-07	
7. Author(s) E. Carson Yates, Jr., Eleanor C. Wynne, Moses G. Farmer, and Robert N. Desmarais				8. Performing Organization Report No.	
9. Performing Organization Name and Address NASA Langley Research Center Hampton, VA 23665				10. Work Unit No.	
				11. Contract or Grant No.	
12. Sponsoring Agency Name and Address National Aeronautics and Space Administration Washington, DC 20546				13. Type of Report and Period Covered Technical Memorandum	
				14. Sponsoring Agency Code	
15. Supplementary Notes This paper was presented at the AIAA Dynamics Specialists Conference, Atlanta, GA, April 9-10, 1981.					
16. Abstract The experiments reported in NASA TM 72837 showed that use of a supercritical airfoil can adversely affect wing flutter speeds in the transonic range. Inasmuch as adequate theories for three-dimensional unsteady transonic flow are not yet available, the modified strip analysis published in NACA RML57L10, (1958) has been used to predict the transonic flutter boundary for the supercritical wing of NASA TM 72837. The steady-state spanwise distributions of section lift-curve slope and aerodynamic center, required as input for the flutter calculations, were obtained from pressure distributions given in NASA TMX-2469. The calculated flutter boundary is in excellent agreement with experiment in the subsonic range. In the transonic range, a "transonic bucket" is calculated which closely resembles the experimental one with regard to both shape and depth, but it occurs at about 0.04 Mach number lower than the experimental one.					
17. Key Words (Suggested by Author(s)) Transonic Flutter Lifting-Surface Flutter Flutter Analysis Modified Strip Analysis			18. Distribution Statement Unclassified-Unlimited Subject Category 39		
19. Security Classif. (of this report) Unclassified		20. Security Classif. (of this page) Unclassified		21. No. of Pages 29	22. Price* A03

End of Document